Dendritic Systems as Active Lewis Acid Catalysts

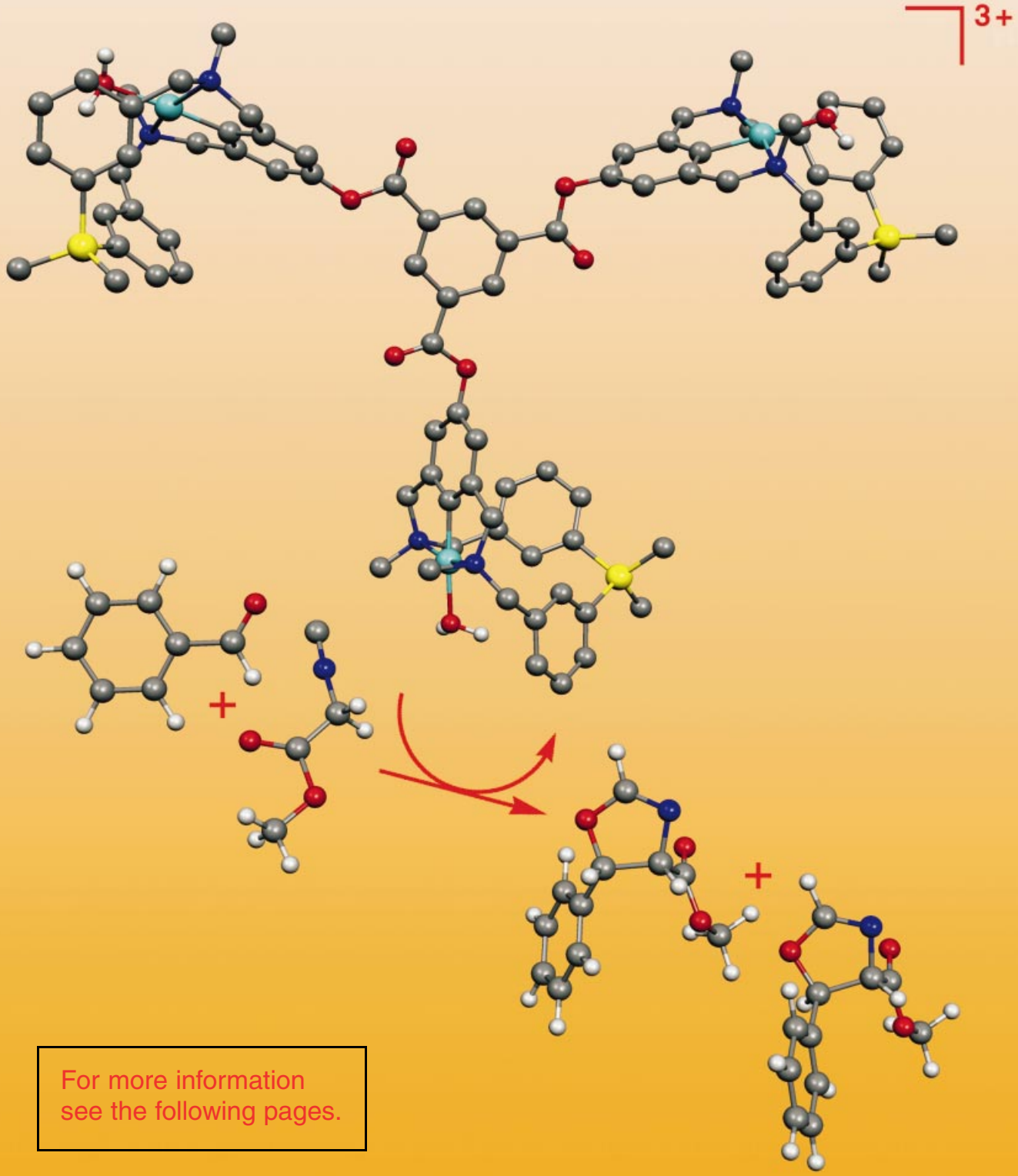

For more information
see the following pages.

  0947-6539/02/0801-0045 $ 17.50+.50/0

New Mono- and Tricyclopalladated Dendritic Systems with Encapsulated Catalytic Sites

Gema Rodríguez,[a] Martin Lutz,[b] Anthony L. Spek,[b] and Gerard van Koten*[a]

Abstract: The preparation of a series of new macrocyclic carbodiazasilane molecules functionalized with the monoanionic $[2,6\text{-}(CH_2NMe_2)_2C_6H_3]^-$ ≡ N,C,N-pincer ligand has been accomplished. Palladation of these systems was possible through oxidative addition with $[Pd(dba)_2]$ affording exclusive formation of the *meso* diastereoisomer. The X-ray crystal structures of these novel ligands and of the palladium(II) complex **10** were determined and confirmed the stereochemistry of the organopalladium cage. Attachment of the *para*-OH functionalized carbodiazasilane macrocycle **16** to a central core led to the formation of the dendritic structure **18** which was palladated to afford the novel multimetallic dendritic system with encapsulated catalytic sites **1**. This cyclopalladated carbosilane dendrimer (**1**) as well as the mononuclear organopalladium cage **10** can be conveniently converted into active Lewis acid catalysts for the aldol condensation reaction. The catalytic data showed higher reaction rates for the dendritic structure than for the corresponding mononuclear systems.

Keywords: cage compounds · catalysts · dendrimers · macrocycles · macrocyclic ligands

Introduction

In the past few years the chemistry of dendrimers has experienced spectacular developments and, very recently, functionalized dendrimers have received substantial attention.[1, 2] In this regard, attractive new materials with interesting chemical, physical and catalytic properties have been prepared consisting of dendrimers or dendritic wedges which contain organometallic functional groups.[3, 4]

One of the most interesting applications of these metallodendrimers is their use in catalysis. Dendrimers having nanoscopic dimensions can be molecularly dissolved. Thus, soluble dendrimers carrying a defined number of catalytic sites can be removed from homogeneous reaction mixtures by simple nanofiltration techniques. The combination of these properties makes them suitable to bridge the gap between homo- and heterogeneous catalysts. Moreover, the use of dendrimers instead of polymers for anchoring catalytic sites leads to well-defined nanosized species in which the number and location of the catalytic sites can be controlled.

In 1994, our group reported on the first carbosilane dendrimer;[5] its periphery is functionalized with catalytic sites based on the monoanionic pincer ligand $[2,6\text{-}(CH_2NMe_2)_2C_6H_3]^-$ (N,C,N).[6] This metallodendritic system was successfully applied as a homogeneous catalyst in organic synthesis and turned out to be suitable for separation by nanomembrane filtration techniques. This multimetallic carbosilane dendrimer was the starting point of our studies in the synthesis and applications of new dendrimers with reactive sites based on N,C,N-pincer and $[2\text{-}(CH_2NMe_2)C_6H_4]^-$ (C,N) ligands.[7]

Over the last five years, numerous metallodendritic catalysts have been reported which contain the catalytically active sites on the outer surface[4, 5, 7, 8] or at the core[9] of the molecule. However, such structures can also have their limitations. Recently, it has been reported that only low generations of peripherally functionalized dendrimers can be suitable carriers of catalytically active sites in atom transfer radical addition reactions.[7a, b] When the catalytic units are placed in a densely packed surface (of a higher generation dendrimer) they can interfere with each other resulting in decreased activity. On the other hand, catalytic sites residing at the core (focal point) of the dendrimer (or dendritic wedge) can be used to change, for example, the solubility properties of the catalyst[10] and it can also result in beneficial interactions between the substrate and the dendritic branches around the catalyst.[11] However, when the catalytic site is located inside a

[a] Prof. Dr. G. van Koten, Dr. G. Rodríguez
Debye Institute, Department of Metal-Mediated Synthesis
Utrecht University, Padualaan 8
3584 CH Utrecht (The Netherlands)
Fax: (+31) 30-2523615
E-mail: g.vankoten@chem.uu.nl

[b] Dr. M. Lutz, Prof. Dr. A. L. Spek[+]
Bijvoet Center for Biomolecular Research
Department of Crystal and Structural Chemistry
Utrecht University, Padualaan 8
3584 CH Utrecht (The Netherlands)
Fax: (+31) 30-2533940
E-mail: a.l.spek@chem.uu.nl

[+] Correspondence pertaining crystallographic studies.

0947-6539/02/0801-0046 $ 17.50+.50/0 *Chem. Eur. J.* **2002**, *8*, No. 1

higher generation dendrimer, the branches can prevent access of the substrate to the reactive center.[12] To date, the introduction of regio- or stereocontrol in a chemical reaction by using dendrimers with an interior isolated catalytic site has not been straightforward. The molecular network of the dendrimers studied have been too flexible and thus unable to impose distinct spatial constraints on the course of the reaction. We therefore considered that progress in this field seems to require specific combinations of dendrimers and encapsulated catalytic sites to encourage regio- and stereocontrol. Following this approach, we set out to develop new multimetallic dendritic systems with catalytically active transition metal complexes placed neither at the periphery nor at the core but encapsulated in a dendritic branch.[13] As a first model, we designed the molecule **1** shown in Figure 1.

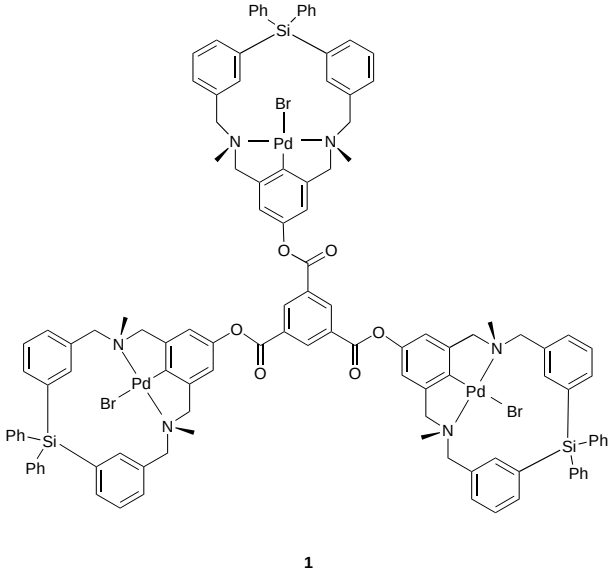

1

Figure 1. Multimetallic dendritic system with encapsulated catalytic sites **1**.

Abstract in Dutch: *Dit onderzoek beschrijft de synthese van een reeks nieuwe, macrocyclische carbodiazasilaan moleculen, die het monoanionisch drievoudig-gecoördineerde tangligand [2,6-$(CH_2NMe_2)_2C_6H_3$]$^-$ ≡ N,C,N bevatten. Deze systemen kunnen door oxidatieve additie met [Pd(dba)$_2$] gepalladeerd worden, waarbij selectief de meso-diastereoisomeren gevormd worden. De structuren van de nieuwe liganden en van het palladium(II)complex **10** zijn kristallografisch onderzocht. Deze kristalstructuuranalyse bevestigt de meso-stereochemie van complex **10**. Het gebruik van de para-OH gefunctionaliseerd macrocyclische carbodiazasilaan verbinding **16** in een convergente synthese-route leidde tot de vorming van de dendritische structuur **18**. Het multi-metallo-dendritische systeem **1** met ingekapselde katalytische centra werd gesynthetiseerd door palladering van verbinding **18**. Het cyclopalladeerde carbosilanedendrimeer **1** en de mononucleaire organopalladium-kooi **10** kunnen eenvoudig omgezet worden in kationische (Lewis zure) centra en zijn getest als katalysatoren in de aldol-condensatiereactie. De katalytische activiteit van de dendritische structuur blijk hoger te zijn dan die van de mononucleaire systemen.*

In this model, the N,C,N-pincer moiety is linked on one side to the core (branching point) and on the other side it is used to coordinate the active metal atom as well as to provide the next branching point (Si) for further extension of the dendritic structure. An interesting aspect of this structure is that **1** has an estimated size of approximately 1.5 nm. Recently we showed that even species of this size could be removed after catalysis from the product-containing solution for reuse by nanomembrane filtration techniques.[7a]

In this paper we report the synthesis of **1** following a convergent procedure compromising first the synthesis of the new macrocyclic carbodiazasilane ligands **8** (see Scheme 2) and the *para*-OH functionalized **16** (see Scheme 5) as the cages, then their attachment to a central core and the subsequent formation of the corresponding palladium(II) complexes by oxidative addition.

We also describe the preliminary results obtained in the use of the aqua complexes of **1** and **10** as homogeneous catalysts using the aldol condensation reaction of benzaldehyde and methyl isocyanoacetate.[14]

Results and Discussion

Synthesis of the macrocyclic carbodiazasilane ligands 8a and 8b: Several approaches to the synthesis of macrocycles have been reported.[15] One of these, described by Kellogg et al.,[16] uses Cs_2CO_3 as a template in an aprotic solvent such as DMF. Depending on the nature of the starting materials, sometimes the use of other salts such as Na_2CO_3 or K_2CO_3 or other solvents such as acetonitrile gave better results. We therefore pursued this strategy to obtain the desired carbodiazasilanes **8** (Scheme 2), utilising the bisbenzylic bromide **5** and the diamines **7a** and **7b**, as precursors (Scheme 1).

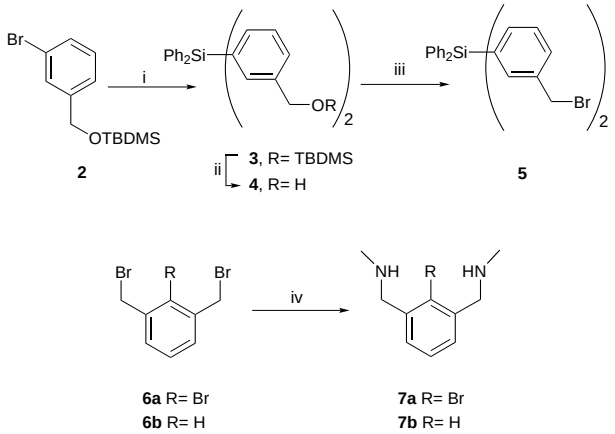

Scheme 1. Synthesis of the bisbenzylic bromide **5** and diamines **7a** and **7b**. i) *t*BuLi, Et_2O, −78 °C, then Ph_2SiCl_2, 12 h; ii) AcOH/THF/H_2O 3:1:1, 50 °C, 3 h; iii) PBr_3, C_6H_6, RT, 3 h; iv) $MeNH_2$, Et_2O, 0 °C, 1.5 h.

Treatment of a solution of 3-bromobenzyl *tert*-butyldimethylsilyl ether (**2**) in diethyl ether with *t*BuLi (2.0 equiv) at −78 °C followed by addition of dichlorodiphenylsilane (0.45 equiv) afforded after work-up the protected benzylic alcohol **3** in good yield (Scheme 1). Deprotection of **3** with a

mixture of AcOH/THF/H_2O 3:1:1 gave rise to the formation of the bisbenzylic alcohol **4** which was easily transformed to the corresponding bisbenzylic bromide **5** by treatment with PBr_3 (0.7 equiv) in benzene at room temperature (81% over two steps). The *meta*-bis(bromomethyl)aryl bromide **6a** and the *meta*-bis(bromomethyl)arene **6b** were prepared according to literature procedures,[17] and subsequently treated with methylamine which afforded the diamines **7a** and **7b**. The building blocks for the synthesis of **8** were then used in the [2 + 2]-macrocyclization reactions shown in Scheme 2. Thus, deprotonation of the bisamino compounds **7a** and **7b** by an alkali metal carbonate followed by reaction of the bisamine with **5** afforded the desired macrocyclic carbodiazasilanes **8a** and **8b**, respectively, by a sequence of two nucleophilic substitutions. Interestingly, formation of dimer **9** was only observed for the reaction of the bisaminoaryl **7a** with **5** (Scheme 2).

Several experimental procedures involving different alkali metal carbonates and solvents were tested in order to establish the best reaction conditions (see Table 1). The best protocol discovered is the dropwise addition of a solution of **5** in DMF to a suspension of **7** and Na_2CO_3 over a period of 2 h

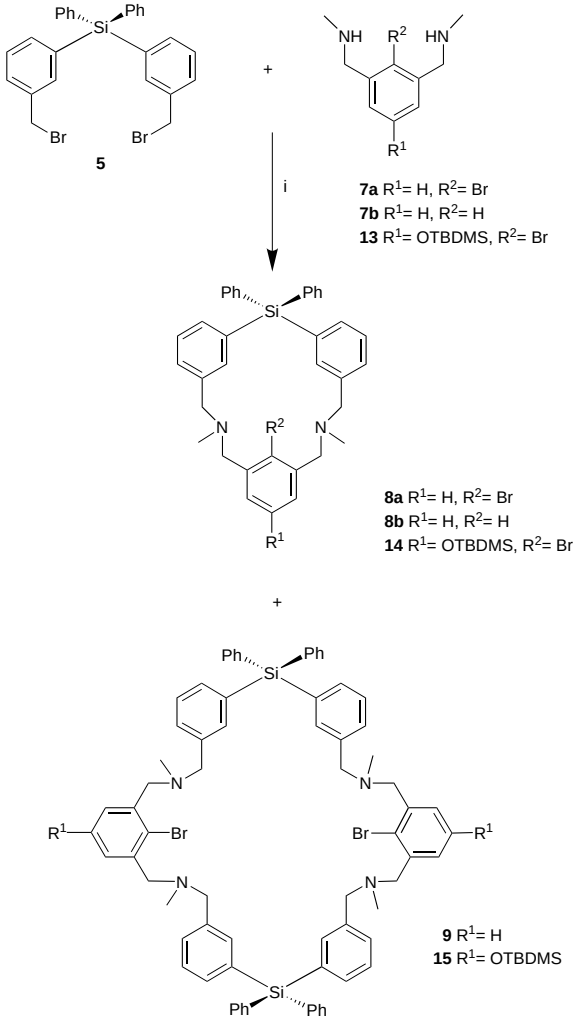

Scheme 2. Synthesis of carbodiazasilane ligands **8a**, **8b** and **14** by a [2+2]-macrocyclization reaction of the benzylic dibromide **5** and diamines **7a**, **7b** and **13**. i) Na_2CO_3, DMF, 50 °C, 14 h.

Table 1. Yields of monomer **8** and dimer **9** using different alkali metal carbonates.[a]

Entry	7	Base	Solvent	Yield [%][b] 8	9	overall
1	**7a**	Cs_2CO_3	DMF	21	12	33
2	**7a**	K_2CO_3	DMF	26	23	49
3	**7a**	Na_2CO_3	DMF	30	16	46
4	**7a**	Na_2CO_3	CH_3CN	8	41	49
5	**7b**	Na_2CO_3	DMF	63	–	63

[a] Reaction conditions: Dropwise addition of a solution of **5** in DMF to a suspension of the metal carbonate and **7** also in DMF, at 50 °C over a period of 2 h. [b] Isolated yield after column chromatography.

(entry 3).[18] The preferred initial concentration of **7** appeared to be 1.3×10^{-2} M. More concentrated solutions gave lower yields of the reaction products. The use of CH_3CN as solvent (entry 4) inverts the ratio monomer (**8**)/dimer (**9**) providing a suitable synthetic route to the dimer **9** in a 41% yield. It is important to note that the absence of bromide, that is the use of the bisaminoarene **7b** as the starting material, leads to the selective formation of the monomer **8b** (entry 5) in a much higher yield than in the corresponding other cases (entries 1 – 4) which most probably is due to steric interference of the bromine atom with the cyclization process.

Synthesis of the palladium(II) complex 10: Reaction of the aryl bromide **8a** with $[Pd(dba)_2]$[19] in refluxing benzene for 12 h gave rise to the formation of the desired macrocyclic Pd^{II} complex **10**, which was isolated as a yellow solid in 47% yield (Scheme 3). However, alternative synthesis from macrocycle **8b**, following electrophilic palladation procedures developed for related hydrocarbons[20] were unsuccessful.

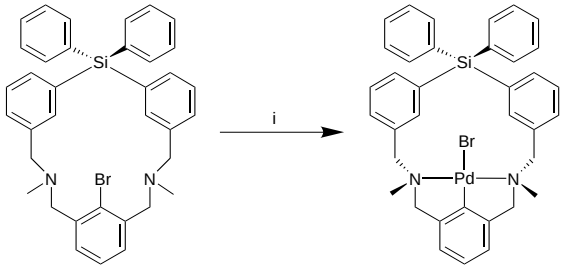

8a **10**

Scheme 3. Transformation of the new carbodiazasilane ligand **8a** into the corresponding Pd^{II} complex **10** by oxidative addition. i) $[Pd(dba)_2]$, C_6H_6, Δ, 12 h.

The structure of **10** was identified on the basis of elemental analysis, MALDI-TOF and ^1H, $^{13}C\{^1H\}$ and two-dimensional NMR spectroscopic data. It is important to note that in **10** the nitrogen atoms are stereogenic centers. As a consequence, four stereoisomers could be formed (*RR*, *SS*, *RS*, *SR*); the *RS* and *SR* forms are identical, when ring flipping of the two fused five membered chelate rings is fast on the NMR time scale, they represent the *meso* compound with an apparent internal mirror plane. The *RR* and *SS* isomers are enantiomers and therefore indistinguishable by ^1H NMR. Therefore, if the palladation reaction of **8a** would give rise to the four possible

0947-6539/02/0801-0048 $ 17.50+.50/0 *Chem. Eur. J.* **2002**, *8*, No. 1

stereoisomers of **10**, two sets of signals should be observed, one attributable to the *meso* compound and one corresponding to the *RR*/*SS* diastereoisomer. Interestingly, the ^{1}H NMR spectrum of complex **10** shows only one group of resonances, indicating the formation of only one diastereomeric form. Definitive proof for the structure of **10** in the solid state was obtained from a single crystal X-ray diffraction study (see below, Figure 3).

Molecular structures of 8a, 8b and 10 in the solid state: To obtain more structural information concerning the conformational preferences of the macrocyclic ring in the arylpalladium compound **10**, the structures of both **10** and the ligands **8a** and **8b** were studied by single crystal X-ray techniques. The molecular geometries of **8a**, **8b** and **10** are shown in Figures 2, 3, respectively, while in Table 2 some pertinent bond lengths and bond and torsion angles have been listed.

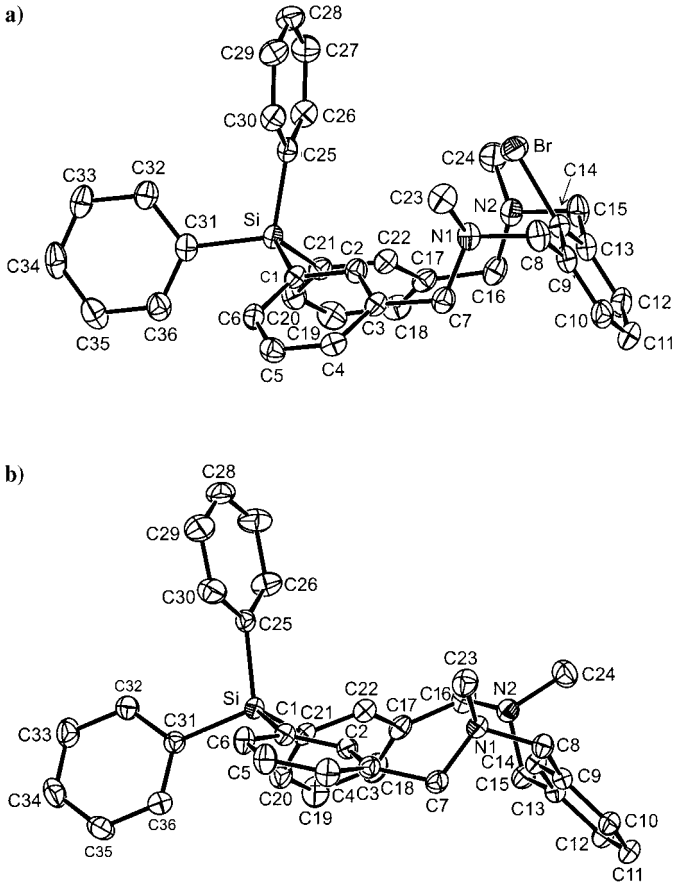

Figure 2. Displacement ellipsoid plots (50% probability) and numbering schemes of the molecular structures of the macrocyclic ligands a) **8a** and b) **8b**. Hydrogen atoms have been omitted for clarity.

The molecular structure of the macrocyclic aryl bromide **8a** (Figure 2a) shows that in the solid state the phenyl groups forming part of the cavity have similar orientations. Thus, protons bound at carbons C2 and C22 which are only 2.38 Å apart from each other and the bromine atom are orientated to the same focal point. The torsion angles for C25-Si-C1-C2 [−56.46(18)°] and C25-Si-C21-C22 [59.52(17)°] indicate similar orientations of the benzylic rings attached to the Si atom. This disposition may be caused by a repulsive effect between the bromine and the two nitrogen atoms. The fixed configuration of the nitrogen centers (*R* and *S* for the N1 and N2, respectively, for the molecule shown[21]) in the solid state (the nitrogen inversion process typical for tertiary amines in solution was not observed) forces the bromine atom to tilt out of the macrocyclic ring and situates the C–Br bond in an assumed suitable disposition to react with $[Pd(dba)_2]$.

A different situation is found in the case of macrocyclic arene **8b**. Although the respective configurations of the nitrogen centers in this molecule are the same as those for these centers in **8a**, the absence of the bromine atom gives more flexibility to the macrocycle. The benzylic rings bonded to the Si atom now exhibit conformations leading to a different orientation of the protons at C2 and C22 (distance 2.54 Å). Likewise, the torsion angles C25-Si-C1-C2 and C25-Si-C21-C22 differ significantly (−98.90(10) and 55.64(11)°, respectively).

The molecular structure of the macrocyclic arylpalladium compound **10** (Figure 3) shows the palladium atom bound to the two nitrogen atoms, to C14 (i.e., C_{ipso} of the monoanionic η^3-N,C,N bonded moiety) and to the bromine atom trans to C_{ipso}. The square-planar coordination geometry is only slightly distorted, in particular the N1-Pd-N2 angle of 161.80(8)°, which is a result of the intrinsically small N-Pd-C14 bite angles of the two neighboring five-membered chelate rings, 81.02(9) and 80.81(9)°, respectively. As a result of the coupled puckering of the two five-membered rings, the N and methyl C atoms are at opposite sides of the plane containing the aryl-Pd portion of the molecule. This puckering conformation is similar to that found for, namely the simple complex $[PdBr(2,6\text{-}\{CH_2NMe_2\}_2C_6H_3)]$.[22]

The two five-membered chelate rings are puckered in such a way that the rest of the macrocycle is orientated perpendicular to the coordination plane. Consequently, several structural features can be observed: i) the bromine atom in **10** is tilted out of the Pd-coordination plane, Br-Pd-C14 174.62(7)°, whereas in other cases such as $1,3,5\text{-}C_6H_3\text{-}[4'\text{-}(PdBr)(2',6'\text{-}\{CH_2NMe_2\}_2C_6H_3)]_3$ this atom is in the coordination plane,[23] ii) one of the methyl groups is in an axial position while the other methyl group is placed equatorially, which is a feature that the structure of **10** has in common with other organoplatinum macrocyclic compounds reported earlier, that is, $[PtI\{CH_2NMe(CH_2)_{10}MeNCH_2C_6H_3\}]$,[24] iii) the aromatic rings from the macrocycle which do not belong to the N,C,N moiety are now orientated in opposite directions. This is in contrast to what is observed for the molecular structure of **8a** in which these aromatic rings are orientated towards the same focal point. However, comparison of conformations of the nitrogen centers in **8a** and **10** show various striking similarities which indicate that these conformations are largely determined by the macrocyclic ring.

NMR Spectroscopy of ligands 8a, 8b and Pd^{II} complex 10: Ligands **8a** and **8b** and arylpalladium complex **10** have been characterized in solution by ^{1}H, ^{13}C{^{1}H} and two-dimensional NMR techniques. The NMR data reveal a high degree of symmetry for these compounds in solution, due to an apparent molecular symmetry plane which contains the

Table 2. Selected bond lengths [Å] and bond and torsion angles [°] for the ligands **8a**, **8b**, **14**, **16** and the Pd^{II} complex **10**.

	8a	8b	10	14	16
bond lengths					
Br−C14	1.905(2)			1.9110(6)	1.9081(17)
N1−C7	1.459(3)	1.4670(15)	1.506(3)	1.458(2)	1.457(2)
N1−C8	1.468(3)	1.4620(15)	1.510(3)	1.457(2)	1.461(2)
N1−C23	1.459(3)	1.4605(15)	1.481(3)	1.460(2)	1.455(2)
C3−C7	1.513(3)	1.5060(16)	1.511(3)	1.513(2)	1.517(2)
C8−C9	1.514(3)	1.5113(16)	1.501(4)	1.509(2)	1.509(2)
C9−C10	1.390(3)	1.3958(16)	1.387(4)	1.390(2)	1.391(2)
C9−C14	1.399(3)	1.3947(16)	1.400(3)	1.400(2)	1.401(3)
Pd−Br			2.5480(3)		
Pd−N1			2.127(2)		
Pd−N2			2.132(2)		
Pd−C14			1.919(2)		
C11−O				1.366(2)	1.357(2)
Si2−O				1.6673(12)	
bond angles					
Br-Pd-N1			100.04(6)		
Br-Pd-N2			97.97(5)		
Br-Pd-C14			174.62(7)		
N1-Pd-N2			161.80(8)		
N1-Pd-C14			81.02(9)		
N2-Pd-C14			80.81(9)		
Pd-N1-C7			109.12(15)		
Pd-N1-C8			107.68(15)		
C7-N1-C8	112.04(16)	109.61(9)	105.67(19)	112.53(13)	113.55(14)
Pd-N2-C15			109.04(14)		
Pd-N2-C16			117.93(15)		
C15-N2-C16	112.49(17)	111.55(10)	110.1(2)	112.78(12)	112.26(13)
O-C11-C10				117.52(15)	117.47(16)
Si2-O-C11				128.32(11)	
torsion angles					
C25-Si-C21-C22	59.52(17)	55.64(11)	91.3(2)	−94.81(15)	83.23(16)
C25-Si-C1-C2	−56.46(18)	−98.90(10)	−159.6(2)	54.45(14)	−48.30(15)
C31-Si-C21-C22	176.27(15)	172.64(9)	−144.6(2)	143.89(14)	−156.17(15)
C31-Si-C1-C2	−174.12(16)	144.49(10)	78.6(2)	176.68(12)	−169.92(13)

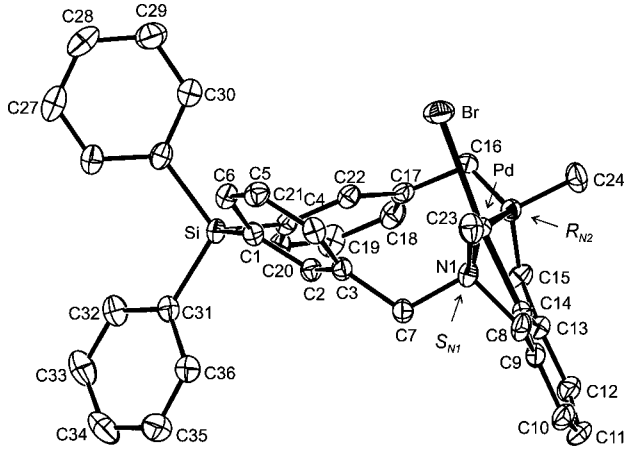

Figure 3. Displacement ellipsoid plot (50% probability) and numbering scheme of the molecular structure of the Pd^{II} complex **10**. Hydrogen atoms have been omitted for clarity.

C14 – C11 axis and the Si atom and it is perpendicular to the C9 – C13 axis (see Figure 2 and Figure 3).

^{1}H NMR spectra: As mentioned above, from the four possible stereoisomers that could be formed in **10** (*RR*, *SS*, *RS*, *SR*) only the *RS*/*SR* pair was observed in the solid state (both *RS* and *SR* pair of enantiomers are present in the unit cell). Formation of the *RR*/*SS* pair is less likely because the aromatic rings of the macrocycle are constrained to one side of the palladium coordination plane, and consequently the methyl groups are positioned at the opposite side. Furthermore, the puckering of the two fused five-membered chelate rings represent another chiral element, which makes the *RS* and *SR* enantiomers unique stereoisomers. However, this is only the case when the chelate ring-flip process is slow on the NMR time scale. When this process becomes fast on the NMR time scale the *RS* and *SR* forms become identical and they then represent the *meso* compound having an internal mirror plane.

The ^{1}H NMR spectrum of the aryl bromide ligand **8a** (300 MHz, CD_2Cl_2, 298 K) shows a singlet for the NMe protons at $\delta = 2.30$ and a very broad signal for the benzylic protons in the range $\delta = 3.20 - 3.80$. The aromatic protons were all found as multiplets between $\delta = 7.12$ and 7.52 except for those bound to C2 and C22 (cf. Figure 2a) which appear as an apparent singlet at $\delta = 7.80$.

On the other hand, in the ^{1}H NMR (300 MHz, CD_2Cl_2, 298 K) of the arene ligand **8b** the resonance for the NMe protons is a singlet at $\delta = 2.24$ while the benzylic protons also appear as a singlet at $\delta = 3.53$. The aromatic region is again characterized by the presence of an apparent singlet at $\delta =$ 8.07 corresponding to the aromatic protons bound to C2 and C22 (cf. Figure 2b) and several multiplets between $\delta = 7.06$ and 7.59.

These NMR data indicate that in the case of **8b**, pyramidal inversion at the nitrogen centers is a fast process on the NMR time scale. Accordingly, the potentially diastereotopic benzylic protons appear as a singlet. The decoalescence of the benzylic protons could not be noted, even at 183 K where only very broad resonances at $\delta = 3.04$, 3.43 and 3.53 for such benzylic protons were observed. This indicates that the inversion of configuration at the nitrogen centers has a very small activation barrier and this process reaches the intermediate exchange rate on the NMR time scale.

A different situation was found for macrocycle **8a**, in which at room temperature broad signals are observed for the protons of the diastereotopic benzylic protons. At low temperatures (203 K) the inversion process at the nitrogen centers is reaching the slow exchange limit shown by the

0947-6539/02/0801-0050 $ 17.50+.50/0 *Chem. Eur. J.* **2002**, *8*, No. 1

observation of two AB patterns at $\delta = 2.14$ and 3.80 and 3.22 and 3.63, respectively, corresponding to the diastereotopic benzylic protons. The presence of the bromine atom in **8a** apparently slows down the inversion process at the nitrogen centers, as this process involves also a movement of the macrocyclic ring.

Evidence for a rigid nitrogen–palladium interaction in the arylpalladium complex **10** on the NMR time scale comes from the observation of diastereotopic resonance patterns of the prochiral methylene protons (^{1}H NMR at 300 MHz, C_6D_6, 298 K). The benzylic protons appear as two AB patterns, protons bound to C7 and C16, at $\delta = 2.87$ and 4.39 while protons bound to C8 and C15 appear at $\delta = 3.03$ and 3.92, respectively (cf. Figure 3). These patterns establish that the nitrogen atoms are stereogenic centers with a stable configuration. This stability arises from the strong Pd–N coordination, which efficiently blocks the inversion process at the nitrogen centers.

Notably **10** exists as stable *RS* and *SR* enantiomers in the solid state. In these stereoisomers, the NMe groups take different positions, that is, one axial and one equatorial, while also the respective protons bound to carbons C2 and C22 have non-equivalent chemical environments. If these distinct orientations were to be maintained in solution, one would expect the ^{1}H NMR spectrum of **10**, for example, to show two resonances for the Me groups and another two for the respective protons bound to carbons C2 and C22. Thus, the chelate ring-flip process involving inversion of the five-membered chelate ring conformations by wagging of the aryl plane about the C11-C14-Pd axis has a low activation barrier and is fast on the NMR time scale.[24b] When low temperature ^{1}H NMR spectra of **10** (300 MHz, CD_2Cl_2, 188 K) were performed, the slow exchange limit for the ring-flip process could not be reached. At 188 K three broad signals for the benzylic protons between $\delta = 3.30$ and 5.00 and a broad singlet at 3.14 for the protons of the methyl group were observed. This spectrum corresponds to the situation in which ring flipping is at an intermediate exchange rate on the NMR time scale.

^{13}C NMR spectra: APT, DEPT and ^{13}C{H^1} NMR experiments were carried out for solutions of the ligands **8a** and **8b** in C_6D_6 and CD_2Cl_2, respectively, while a ^{1}H,^{13}C COSY spectrum was also obtained from a solution of complex **10** in C_6D_6, in order to assign all signals. Although for macrocycles **8a** and **8b** the ^{13}C NMR data reveal high symmetry, a different result is observed for compound **10**. The ^{13}C NMR of the arylpalladium macrocycle **10** shows six signals for tertiary carbons and another two for quaternary carbons corresponding to the phenyl rings bound to the silicon atom which do not belong to the macrocycle. This result is not only further evidence for the strong Pd–N coordination, which blocks the inversion process at the nitrogen centers, but also reveals that part of the 12-membered macrocycle, which does not include the N,C,N moiety, is now orientated perpendicular to the coordination plane (cf. Figure 3). As a result, the two phenyl rings of the Ph_2Si moiety have also now become diastereotopic, that is, the 12-membered macrocycle has a distinct puckering at this temperature.

Synthesis and characterization of the multimetallic dendritic system 1: Having optimized the conditions for the synthesis of the metallic cage **10**, we pursued the synthesis of the desired dendrimer **1** following a convergent procedure. For the coupling of this cage to the core benzenetricarbonyl trichloride **17** we prepared the new functionalized cage **16** with a phenol group as a binding site (Scheme 5). For the synthesis of the macrocycle **16** the same synthetic procedure was used as for the synthesis of ligands **8**, that is, a [2 + 2]-macrocyclization reaction between the bisbenzylic bromide **5** and the bisaminoaryl bromide **13** (see Scheme 2). Compound **13** was prepared following the route shown in Scheme 4. Treatment of a solution of **11**[7g] in methanol with $PyH \cdot Br_3$ (1 equiv) in the presence of iron powder afforded the brominated bisbenzylic alcohol **12**.[25] Reaction of **12** with mesyl chloride using Et_3N as a base followed by nucleophilic attack of methylamine on the resulting mesylate led to the bisamine **13** (88% yield, two steps).

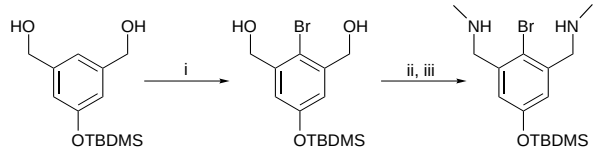

11 **12** **13**

Scheme 4. Synthesis of diamine **13**. i) $PyH \cdot Br_3$, Fe powder, CH_2Cl_2, RT, 1 h; ii) MsCl, Et_3N, CH_2Cl_2, $-78\,^\circ$C, 1.5 h; iii) $MeNH_2$, Et_2O, $-78\,^\circ$C, 1 h.

The [2 + 2]-macrocyclization reaction between compounds **5** and **13** was carried out following the best protocol found for the preparation of ligands **8a** and **8b** (see above). Thus, dropwise addition of a solution of **5** in DMF to a suspension of **13** and Na_2CO_3 also in DMF over a period of 2 h afforded the desired carbodiazasilane ligand **14** and the dimer **15** in a 30% and 4% yield, respectively (Scheme 2). When this reaction was performed using K_2CO_3 as a base in addition to monomer **14** and dimer **15**, formation of the deprotected phenol **16** was also observed. Further deprotection of macrocycle **14** to yield the *para*-functionalized carbodiazasilane ligand **16** took place by treatment of a solution of **14** in THF with tetrabutylammonium fluoride (1.3 equiv) for 1 h (Scheme 5).

Molecular structures of 14 and 16: Unequivocal confirmation of the proposed connectivity was obtained from single crystal structure determinations of **14** and **16** (see Figure 4 and Table 2). The overall structural features of **14** were expected to be similar to those found for macrocycle **8a**. However, the configuration of one of the nitrogen centers in **14** is different than in **8a** thus, the two nitrogen centers in **14** have the same configuration *S* and therefore the benzylic rings in this molecule have a different orientation than in **8a** (torsion angles for C25-Si-C1-C2 and C25-Si-C21-C22 are 54.45(14) and $-94.81(15)^\circ$, respectively).

In the solid state, ligand **16** forms dimers resulting from the formation of intermolecular hydrogen bonds between the phenolic hydrogen atom and one of the nitrogen atoms of the adjacent molecule. This hydrogen bonding brings about a

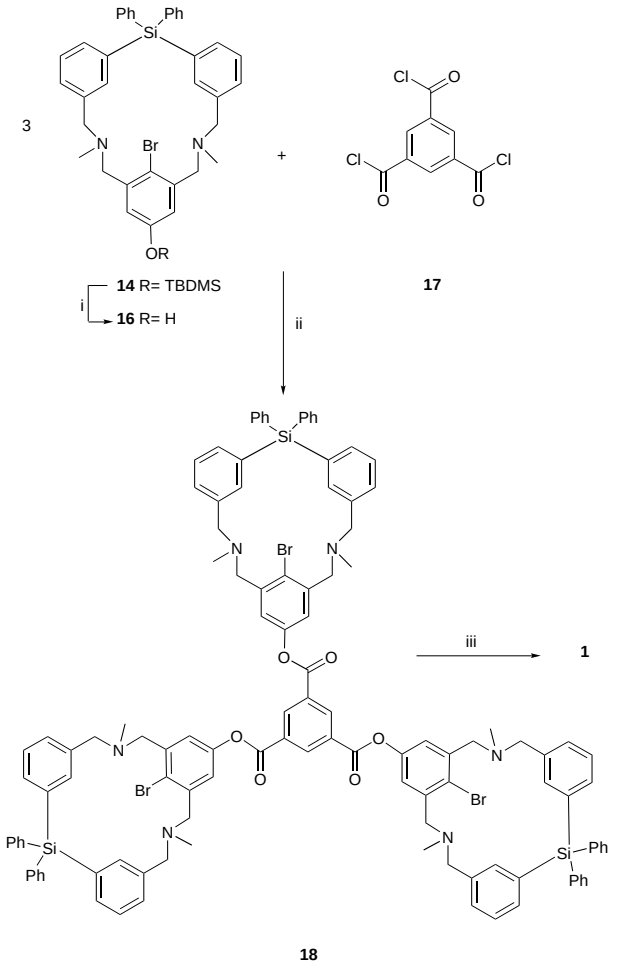

Scheme 5. Synthesis of the multimetallic dendritic system **1**. i) Bu_4NF, THF, RT, 1 h; ii) Et_3N, THF, RT, 12 h; iii) $Pd(dba)_2$, toluene, Δ, 12 h.

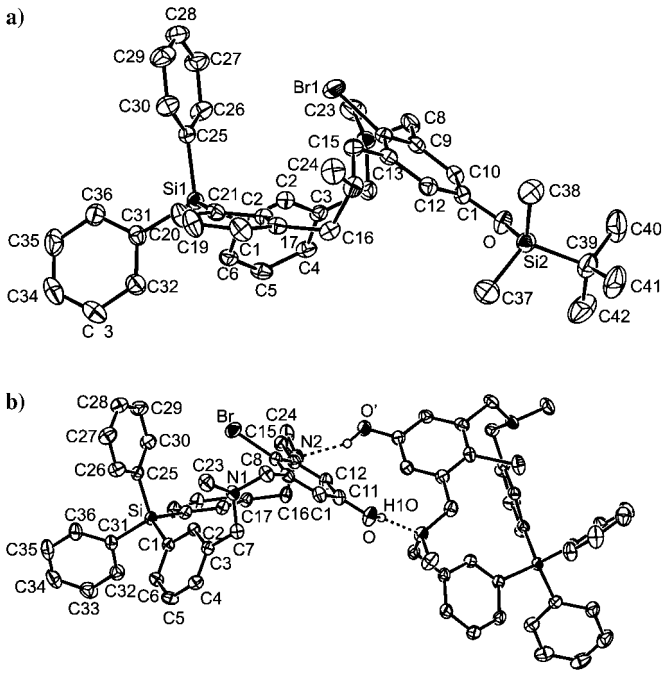

Figure 4. Displacement ellipsoid plots (50% probability) and numbering schemes of the structures of the macrocyclic ligands a) **14** and b) the hydrogen bonded dimer of **16**. Hydrogen atoms have been omitted for clarity, except H1O in **16**.

change in the configuration of the nitrogen centers relative to those in the bromine ligand **8a** (N1 and N2 have *R* and *S* configuration in **8a**, respectively, while the configuration in **16** for N1 is *R* and for N2 is *S*). Therefore, the disposition of the benzylic rings attached to the Si atom in **14** is again not comparable to the one in **8a** (torsion angles for C25-Si-C1-C2 and C25-Si-C21-C22 are $-48.30(15)$ and $83.23(16)^\circ$, respectively).

We attempted the palladation of ligands **14** and **16** by oxidative addition to $[Pd(dba)_2]$. Unfortunately, when the respective solutions of the carbodiazasilanes **14** and **16** in benzene were heated under reflux overnight in the presence of $[Pd(dba)_2]$ the desired palladated species were not formed and only starting material could be recovered. Attempts to increase the reactivity of these compounds by using other solvents such as toluene or 1,2-dichlorobenzene failed. The low reactivity of macrocycles **14** and **16** compared with that of ligand **8a** is probably due to the presence of an electron donating group in the N,C,N moiety. Therefore, we decided to prepare the dendritic compound **18** (Scheme 5) in order to obtain cages functionalized with more electron withdrawing groups, such as ester moieties, expecting to have a more reactive system towards palladation. Treatment of a solution of freshly recrystallized 1,3,5-benzenetricarbonyl chloride (**15**) in THF with the phenolic ligand **16** (3.5 equiv), in the presence of Et_3N afforded the dendritic molecule **18** in an 88% yield. The ^1H NMR spectrum of **18** shows a similar pattern to that observed for compound **16** with the most remarkable difference being the singlet at $\delta = 9.50$ corresponding to the three aromatic protons of the triester core.

The final step in the synthesis of **1** was the palladation reaction of **18** which indeed took place readily by oxidative addition to $[Pd(dba)_2]$. Thus, refluxing of a solution of the multicage dendritic system **18** in toluene overnight in the presence of $[Pd(dba)_2]$ gave rise to **1** as a yellow solid in a 60% yield. A notable feature of **1** is the two diagnostic downfield singlets in the ^1H NMR spectrum which are assigned to the three protons of the central aromatic triester ring ($\delta = 9.44$) and to the hydrogens bound to C2 and C22 ($\delta = 10.00$, cf. Figure 3), respectively.

Molecular mechanics calculations[26] suggest that the overall geometry of dendrimer **1** is best described as a helix (see Figure 5). The average distance between two of the three palladium centers of **1** is ≈ 1.5 nm. Although this molecule has a fairly low molecular weight of 2334 Da its helical structure gives it true nanoparticle size dimensions and thus, appropriate properties for retainment by (nano)membrane filtration materials.[27]

Catalysis: The macrocyclic Pd^{II} complex **10** and dendrimer **1** were used as catalyst precursors in the aldol condensation reaction of benzaldehyde and methyl isocyanoacetate to form oxazolines (Scheme 6). Their catalytic preformance was compared with the activity of the corresponding mononuclear and model compounds $[PdBr(2,6\text{-}\{CH_2NMe_2\}_2C_6H_3)]$ (**19**), $[PdI(4\text{-}CO_2Me\text{-}2,6\text{-}\{CH_2NMe_2\}_2C_6H_2)]$ (**20**) and $[PdBr(2,6\text{-}\{CH_2NMeBn\}_2C_6H_3)]$ (**21**).

Consequently, **1**, **10**, **19**, **20** and **21** were converted in their corresponding (poly)cationic analogues by abstracting the

0947-6539/02/0801-0052 $ 17.50+.50/0 *Chem. Eur. J.* **2002**, *8*, No. 1

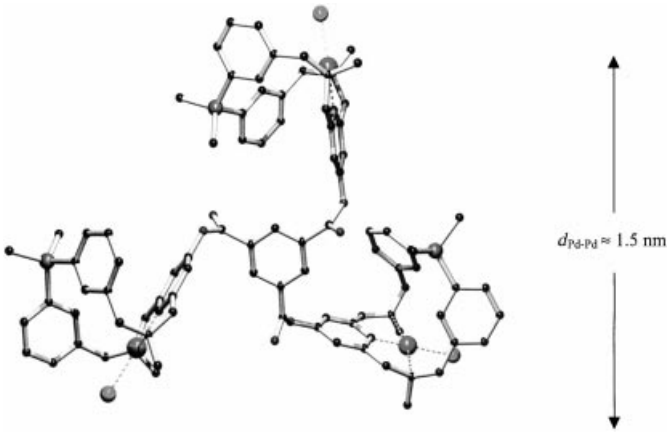

Figure 5. Molecular modelling structure of **1** (MMFF94).

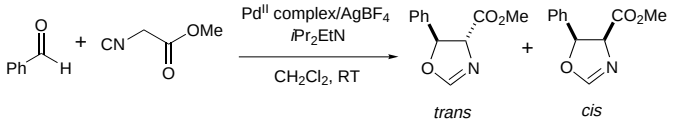

Scheme 6. Aldol condensation reaction of benzaldehyde and methyl isocyanoacetate yielding oxazolines.

halide anion using $AgBF_4$ in wet acetone.[28] After appropiate work-up involving a thorough filtration of the solutions containing the cationic complexes through a path of Celite to remove the insoluble silver halide salts[29] active catalytic species were isolated and used without further purification in the aldol condensation reaction.

These preliminary experiments were carried out with iPr_2EtN (Huenig's base, 10 mol%) as a base, using 1 mol% of the catalyst, methyl isocyanoacetate (100 mol%) and benzaldehyde (100 mol%) in dichloromethane at room temperature. The results obtained with different Pd^{II} complexes are shown in Table 3.

The polycationic dendritic system derived from **1** turned out to have a higher catalytic activity than the other mononuclear model compounds tested (entry 2). The presence of an ester moiety at the *para*-position of the catalytic site seems to play an important role in the activity of these systems (entries 3 and 4). An interesting difference on the reaction rate was noted between compounds **19** and **21** (entries 3 and 5). Apparently the alkyl substituents at the nitrogen centers seem to influence the reactivity of these catalysts for the acyclic compounds. Interestingly, this decrease in the reaction rate is not observed for the case of the cyclic analogue **10** (entry 1) demonstrating the positive influence of the cage. Unfortunately, the steric environment around the Pd site caused by the presence of the cavity in **10** does not have an influence on the diastereoselectivity of the reaction.

Table 3. Aldol condensation reaction of methylisocyanate and benzaldehyde.[a, b]

Entry	Pd^{II} complex	Time [h]	Conversion[b] [%]	*trans*/*cis*[b]
1	**10** (Pd_1 species)	7	89	71/29
2	**1** (Pd_3 species)	4	>99	61/39
3	[PdBr(2,6-{CH_2NMe_2}$_2$$C_6H_3$)] (**19**)	7	83	62/38
4	[PdI(4-CO_2Me-2,6-{CH_2NMe_2}$_2$$C_6H_2$)] (**20**)	7	>99	62/38
5	[PdBr(2,6-{CH_2NMeBn}$_2$$C_6H_3$)](**21**)	7	40	63/37

[a] Reaction carried out in CH_2Cl_2 (5 mL) at RT with ca. 10 mol% Hüning's base [Et(*i*Pr)$_2$N]. [b] In all catalytic rounds the amount of palladium was kept constant (i.e., ca. 1 mol%). [c] Conversion and *trans*/*cis* ratio calculated using specific signal integration in the ^{1}H NMR spectra.

Conclusion

In the present investigation, we have developed the synthesis of two new macrocyclic carbodiazasilane molecules containing the monoanionic N,C,N-ligand **8a** and **8b**. Macrocycle **8a** was successfully transformed to the organometallic Pd^{II} complex **10** by oxidative addition to [Pd(dba)$_2$]. A remarkable aspect in the synthesis of complex **10** is the formation of only the *meso* compound from all the possible stereoisomers.

Modification of the macrocycles **8a** by introduction of a phenol group at the *para*-position of the N,C,N moiety afforded the ligands **14** and **16**. The attachment of cage **16** to a central core gave rise to the novel multicage dendritic structure **18** which was palladated in order to obtain the novel multimetallic dendrimer **1**. The cationic derivative of **1** obtained by halide abstraction with $AgBF_4$ was successfully applied as homogeneous catalyst showing higher reaction rates than the mononuclear analogues.

Experimental Section

General: All sensitive manipulations were performed under a dry and deoxygenated dinitrogen atmosphere using standard Schlenk techniques unless otherwise stated. All solvents were carefully dried and distilled prior to use. All standard chemicals were purchased from Acros Chimica or Aldrich and used without further purification. 1,3,5-Benzenetricarboxylic acid chloride was recrystallized from hot hexanes prior to use. Flash chromatography was performed using 230–400 mesh silica (Merck). The starting materials 1,3-bis(hydroxymethylbenzene) *tert*-butyldimethylsilyl ether,[30] [Pd$_2$(dba)$_2$],[19b] **19**[19,24a] and **20**[31] were synthesized according to literature procedures. ^{1}H (200 or 300 MHz), ^{13}C (50 or 75 MHz) and ^{29}Si (75 MHz) NMR spectra were recorded on a Varian Inova spectrometer. Chemical shifts are given in ppm using TMS as an external standard. Elemental analyses were performed by Dornis and Kolbe, Mikroanalytisches Laboratorium (Mülheim a.d. Ruhr, Germany). MALDI-TOF-MS spectra were acquired using a Voyager-DE BioSpectrometry Workstation (PerSeptive Biosystems Inc., Framingham, MA) mass spectrometer equipped with a nitrogen laser emitting at 337 nm. The instrument was operated in the linear mode at an accelerating voltage in the range 22000 V. External calibration was performed using C_{60}/C_{70}, and detection was performed by means of a linear detector and digitizing oscilloscope operating at 500 MHz. Sample solutions with $\approx$10 mg mL^{-1} in THF were used, and the matrix was 3,5-dihydroxybenzoic acid in THF (10 mg mL^{-1}). A solution of silver(I) trifluoroacetate in THF was added to the sample in order to improve the peak resolution. The sample solution (0.2 μL) and the matrix solution (0.2 μL) were combined and placed on a gold MALDI target and analyzed after evaporation of the solvents.

$Ph_2Si(C_6H_4CH_2OSiMe_2tBu)_2$ (3): A sample of 3-bromobenzyl *tert*-butyldimethylsilyl ether (**2**) (20.15 g, 66.87 mmol) was dissolved in Et_2O (250 mL) and the solution cooled to $-78\,^\circ$C. *tert*-Butyllithium (85 mL of a 1.5 M solution in pentane, 127.06 mmol) was added dropwise and the mixture was stirred for 30 min, followed by the addition of dichlorodiphenylsilane (7.62 g, 6.33 mL, 30.09 mmol). The yellow suspension was allowed to warm slowly to room temperature and then stirred overnight. To the resulting white suspension was added an extra amount of *t*BuLi (4.25 mL). After stirring for 10 min, the reaction mixture was quenched with a saturated

aqueous solution of NH_4Cl until a clear two-phase system was obtained. The aqueous layer was separated and washed with Et_2O (2×100 mL). The combined organic layers were washed with H_2O (2×50 mL) and brine (50 mL), and then dried over $MgSO_4$. This solution was filtered and reduced under vacuum to a crude yellow oil, which was purified by flash column chromatography (EtOAc/hexanes 1:2). The product was obtained as a colorless oil (16.36 g, 87%). ^{1}H NMR (300 MHz, C_6D_6, 25 °C): $\delta = -0.03$ (s, 12H; $SiMe_2$), 0.89 (s, 18H; Si*t*Bu), 4.52 (s, 4H; ArCH_2), 7.13–7.24 (m, 8H; Ar*H*), 7.39 (d, ^3J(H,H) = 7.8 Hz, 2H; ArH), 7.62 (d, ^3J(H,H) = 7.2 Hz, 2H; Ar*H*), 7.70–7.74 (m, 4H; Ar*H*), 7.78 (s, 2H; Ar*H*); ^{13}C NMR (50 MHz, C_6D_6, 25 °C): $\delta = -5.10$ ($SiMe_2$), 18.5 [Si*C*$(CH_3)_3$], 26.18 [SiC(CH_3)$_3$], 65.15 (ArCH_2), 127.81, 128.28, 128.32, 129.88, 134.42, 134.71 (C), 134.92 (C), 135.62, 136.92, 141.36 (C); ^{29}Si NMR (75 MHz, C_6D_6, 25 °C): $\delta = -13.3$ (Ar_2Si), 20.0 (*Si*O); MS (MALDI-TOF): *m*/*z*: calcd for: 732.9; found: 732.8 $[M+Ag]^+$; elemental analysis calcd (%) for $C_{38}H_{52}O_2Si_3$ (625.07): C 73.02, H 8.39, Si 13.48; found C 73.10, H 8.49, Si 13.57.

$Ph_2Si(C_6H_4CH_2OH)_2$ (4): A solution of **3** (3.53 g, 5.65 mmol) in a mixture of AcOH/THF/H_2O (3:1:1, 30 mL) was warmed to 50 °C and stirred for 3 h. After this time, the reaction mixture was cooled to room temperature and all volatiles were removed in vacuo. The residue obtained was dissolved in Et_2O (30 mL) and an aqueous solution of NaOH (1M) was added until neutral pH was reached. The organic layer was separated, washed with H_2O (2×10 mL) and brine (1×10 mL), and then dried over $MgSO_4$. This solution was filtered and the volatiles were removed in vacuo to yield a crude yellow oil, which was purified by flash column chromatography (EtOAc/hexanes 2:1). The product was obtained as a colorless oil (1.99 g; 89%). ^{1}H NMR (200 MHz, C_6D_6, 25 °C): $\delta = 3.39$ (brs, 2H; O*H*), 4.20 (s, 4H; ArCH_2), 7.04–7.18 (m, 10H; Ar*H*), 7.57 (d, ^3J(H,H) = 6.2 Hz, 2H; Ar*H*), 7.66–7.69 (m, 4H; Ar*H*), 7.76 (s, 2H; Ar*H*); ^{13}C NMR (50 MHz, C_6D_6, 25 °C): $\delta = 64.83$ (ArCH_2), 128.37, 128.43, 128.90, 129.99, 134.75 (C), 134.82 (C), 135.24, 135.90, 136.89, 141.33 (C); FAB-MS: *m*/*z*: 396.1 $[M]^+$; elemental analysis calcd (%) for $C_{26}H_{24}O_2Si$ (396.55): C 78.75, H 6.10, Si 7.08; found C 78.64, H 6.14, Si 7.02.

$Ph_2Si(C_6H_4CH_2Br)_2$ (5): A solution of PBr_3 (0.94 g, 3.45 mmol) in benzene (10 mL) was slowly added (15 min) to a solution of **4** (1.99 g, 4.97 mmol) in benzene (20 mL) at room temperature. After stirring the reaction mixture for 3 h, the solvent was removed in vacuo. The residue obtained was purified by flash column chromatography (EtOAc/hexanes 0.25:9.75) to afford the desired bisbenzyl bromide **7** as a colorless oil (2.13 g, 91%). ^{1}H NMR (300 MHz, C_6D_6, 25 °C): $\delta = 3.87$ (s, 4H; ArCH_2), 7.02 (t, ^3J(H,H) = 7.2 Hz, 2H; Ar*H*), 7.10–7.22 (m, 8H; Ar*H*), 7.47–7.50 (m, 2H; Ar*H*), 7.60–7.63 (m, 6H; Ar*H*); ^{13}C NMR (50 MHz, C_6D_6, 25 °C): $\delta = 33.41$ (ArCH_2), 128.45, 128.75, 130.21, 130.90, 134.00 (C), 135.23 (C), 136.71, 136.80, 137.00, 138.10 (C); ^{29}Si NMR (75 MHz, C_6D_6, 25 °C): $\delta = -13.59$; FAB-MS: *m*/*z*: 521/523/525 $[M+H]^+$; elemental analysis calcd (%) for $C_{26}H_{22}Br_2Si$ (522.35): C 59.78, H 4.25, Si 5.38; found C 59.72, H 4.18, Si 5.41.

1-Bromo-2,6-bis[(methylamino)methyl]benzene (7a): A solution of 2-bromo-1,3-bis(bromomethyl)benzene (**6a**) (2.07 g, 6.04 mmol) in Et_2O (20 mL) was cooled to 0 °C. $MeNH_2$ was bubbled through this solution for a period of 4 min. The reaction mixture was then stirred for 20 min and $MeNH_2$ gas was again bubbled through the reaction for 4 min. Formation of a white precipitate was observed. The suspension was allowed to warm to room temperature and stirred for 1 h. After this time, water was added and the organic layer was separated. The obtained organic layer was washed with brine (10 mL), dried over $MgSO_4$ and concentrated to afford the desired diamine **7a** as a yellow oil (1.00 g, 68%). ^{1}H NMR (200 MHz, C_6D_6, 25 °C): $\delta = 0.92$ (brs, 2H; N*H*), 2.21 (brs, 6H; NCH_3), 3.74 (brs, 4H; ArCH_2), 7.05 (t, ^3J(H,H) = 5.0 Hz, 2H; Ar*H*), 7.23 (d, ^3J(H,H) = 5.0 Hz, 1H; Ar*H*); ^{13}C NMR (75 MHz, $CDCl_3$, 25 °C): $\delta = 35.73$ (NCH_3), 56.11 (ArCH_2), 125.57 (C), 126.94, 128.95, 139.46 (C).

Synthesis of ligands 8a and 9: The following is an example of the experimental conditions used for the performance of the [2+2]-macrocyclization reaction. A suspension of 2-bromo-1,3-bis[(methylamino)methyl]benzene (0.19 g, 0.80 mmol) and Na_2CO_3 (0.21 g, 2.01 mmol) in DMF (60 mL) was stirred for 15 min at 50 °C. A solution of **5** (0.42, 0.80 mmol) in DMF (20 mL) was then added dropwise over 2 h and the reaction mixture was stirred overnight at this temperature. DMF was removed in vacuo and the crude product was dissolved in CH_2Cl_2 (80 mL). The organic layer was washed with H_2O (2×40 mL) and brine (2×40 mL), dried over $MgSO_4$, filtered and concentrated. The residue obtained was purified by flash column chromatography (EtOAc/hexanes 1:4) to afford two products: the desired macrocycle **8a** (0.14 g, 30%) and the dimer **9** (20 mg, 4%). Macrocycle **8a**: ^{1}H NMR (300 MHz, CD_2Cl_2, 25 °C): $\delta = 2.30$ (s, 6H; NCH_3), 3.20–3.80 (brm, 8H; ArCH_2), 7.12–7.23 (m, 6H; Ar*H*), 7.29–7.52 (m, 13H; Ar*H*), 7.80 (s, 2H; Ar*H*); ^{1}H NMR (300 MHz, C_6D_6, 25 °C): $\delta = 2.20$ (s, 6H; NCH_3), 3.10–3.70 (brm, 8H; ArCH_2), 6.89–6.94 (m, 1H; Ar*H*), 7.02–7.21 (m, 12H; Ar*H*), 7.57 (d, ^3J(H,H) = 6.9 Hz, 2H; Ar*H*), 7.66–7.73 (m, 4H; Ar*H*), 8.09 (s, 2H; Ar*H*); ^{13}C NMR (75 MHz, C_6D_6, 25 °C): $\delta = 42.48$ (NCH_3), 58.36 (ArCH_2), 61.75 (ArCH_2), 126.05, 127.44, 128.10 (C), 128.88 (C), 129.72, 130.07, 130.42, 135.04, 135.34 (C), 137.21 (2 × ArH), 137.56, 138.78 (C), 140.24 (C); ^{29}Si NMR (75 MHz, C_6D_6, 25 °C): $\delta = -14.47$; MS (MALDI-TOF): m/z: calcd for: 603.7; found: 603.3 $[M]^+$, 523.7 $[M - Br]^+$; elemental analysis calcd (%) for $C_{36}H_{35}BrN_2Si$ (603.67): C 71.63, H 5.84, N 4.64, Si 4.65; found C 71.80, H 5.76, N 4.54, Si 4.55.

Dimer **9**: ^{1}H NMR (300 MHz, C_6D_6, 25 °C): $\delta = 2.00$ (s, 12H; NCH_3), 3.36 (s, 8H; ArCH_2), 3.55 (s, 8H; ArCH_2), 6.99 (t, ^3J(H,H) = 7.5 Hz, 2H; Ar*H*), 7.16–7.22 (m, 16H; Ar*H*), 7.31 (d, ^3J(H,H) = 7.8 Hz, 4H; Ar*H*), 7.39 (d, ^3J(H,H) = 7.5 Hz, 4H; Ar*H*), 7.65 (d, ^3J(H,H) = 7.2 Hz, 4H; Ar*H*), 7.75–7.79 (m, 8H; Ar*H*), 7.93 (s, 4H; Ar*H*); ^{13}C NMR (75 MHz, C_6D_6, 25 °C): $\delta = 42.18$ (NCH_3), 61.81 (ArCH_2), 62.41 (ArCH_2), 126.72 (C), 127.16, 127.91, 128.34, 129.19, 129.90, 130.60, 134.84 (C), 135.05 (C), 135.66, 136.96, 137.40, 139.29 (C), 139.37 (C); ^{29}Si NMR (75 MHz, C_6D_6, 25 °C): $\delta = -13.46$; MS (MALDI-TOF): *m*/*z*: calcd for 1207.3; found: 1207.6 $[M]^+$, 1128.0 $[M - Br]^+$; elemental analysis calcd (%) for $C_{72}H_{70}Br_2N_4Si_2$ (1207.3): C 71.63, H 5.84, N 4.64, Si 4.65; found C 71.41, H 5.98, N 4.39, Si 4.48.

Synthesis of macrocycle 8b: This compound was prepared as described for **8a**, starting from **7b** in 63% yield as a white solid. ^{1}H NMR (300 MHz, CD_2Cl_2, 25 °C): $\delta = 2.24$ (s, 6H; NCH_3), 3.53 (s, 8H; ArCH_2), 7.07 (d, ^3J(H,H) = 7.5 Hz, 2H; Ar*H*), 7.18–7.23 (m, 1H; Ar*H*), 7.30–7.49 (m, 12H; Ar*H*), 7.56–7.59 (m, 5H; Ar*H*), 8.07 (s, 2H; Ar*H*); ^{1}H NMR (200 MHz, C_6D_6, 25 °C): $\delta = 2.05$ (s, 6H; NCH_3), 3.32 (s, 4H; ArCH_2), 3.41 (s, 4H; ArCH_2), 6.96 (d, ^3J(H,H) = 7.4 Hz, 4H; Ar*H*), 7.10–7.20 (m, 9H; Ar*H*), 7.62–7.65 (m, 2H; Ar*H*), 7.72–7.76 (m, 4H; Ar*H*), 7.96 (s, 1H; Ar*H*), 8.42 (s, 2H; Ar*H*); ^{13}C NMR (75 MHz, CD_2Cl_2, 25 °C): $\delta = 43.12$ (NCH_3), 60.72 (ArCH_2), 61.77 (ArCH_2), 128.00, 128.04, 128.16, 128.44, 129.01 (C), 130.14, 131.24, 134.91 (C), 135.23 (C), 135.68, 136.98, 137.12, 139.72 (C); MS (MALDI-TOF): *m*/*z*: calcd for: 524.8; found: 524.0 $[M]^+$; elemental analysis calcd (%) for $C_{36}H_{36}N_2Si$ (603.67): C 82.40, H 6.91, N 5.34, Si 5.35; found C 82.46, H 6.85, N 5.28, Si 5.29.

Synthesis of the Pd^{II} complex 10: [Pd(dba)$_2$] (66 mg, 0.11 mmol) was added to a solution of **8a** (63 mg, 0.10 mmol) in benzene (5 mL). The resulting solution was refluxed overnight, during which time the color changed from deep purple to yellow. The reaction mixture was filtered through Celite and the solvent removed under reduced pressure. The solid residue was dissolved in wet acetone (8 mL) and $AgBF_4$ (21 mg, 0.11 mmol) was added, the suspension was stirred for 1 h. After this time, the resulting cloudy suspension was filtered through Celite, and the solvent was concentrated to ca. 2 mL. Et_2O was added to this solution in order to precipitate the product. The precipitate was purified by washing several times with Et_2O. The precipitate was then dissolved in CH_2Cl_2 and an excess of LiBr was added to the solution, which was stirred for 2 h. Filtration of the suspension through Celite and revomal of the solvent in vacuo afforded compound **10** which was isolated as an air and temperature-stable yellow crystalline solid (35 mg, 47%). ^{1}H NMR (300 MHz, CD_2Cl_2, 25 °C): $\delta = 3.21$ (s, 6H; NCH_3), 3.40 (d, ^3J(H,H) = 11.8 Hz, 2H; ArCH_2), 3.63 (d, ^3J(H,H) = 14.8 Hz, 2H; ArCH_2), 4.23 (d, ^3J(H,H) = 14.8 Hz, 2H; ArCH_2), 4.50 (d, ^3J(H,H) = 11.8 Hz, 2H; ArCH_2), 6.70 (d, ^3J(H,H) = 7.5 Hz, 2H; Ar*H*), 6.88 (m, 1H; Ar*H*), 7.28–7.59 (m, 16H; Ar*H*), 9.58 (s, 2H; Ar*H*); ^{1}H NMR (300 MHz, C_6D_6, 25 °C): $\delta = 2.87$ (d, ^3J(H,H) = 12.0 Hz, 2H; ArCH_2), 2.91 (s, 6H; NCH_3), 3.03 (d, ^3J(H,H) = 14.6 Hz, 2H; ArCH_2), 3.92 (d, ^3J(H,H) = 14.6 Hz, 2H; ArCH_2), 4.39 (d, ^3J(H,H) = 12.0 Hz, 2H; ArCH_2), 6.46 (d, ^3J(H,H) = 7.5 Hz, 2H; Ar*H*), 6.80 (t, ^3J(H,H) = 7.4 Hz, 1H; Ar*H*), 6.87 (d, ^3J(H,H) = 7.5 Hz, 2H; Ar*H*), 7.06–7.25 (m, 8H; Ar*H*), 7.69 (d, ^3J(H,H) = 7.2 Hz, 4H; Ar*H*), 7.87–7.90 (m, 2H; Ar*H*), 10.09 (s, 2H; Ar*H*); ^{13}C NMR (50 MHz, C_6D_6, 25 °C): $\delta = 52.49$ (NCH_3), 66.97 (ArCH_2), 69.71 (ArCH_2), 119.79, 124.35, 127.60, 128.34, 128.44, 129.90, 129.99, 133.24, 134.01 (C), 134.77 (C), 134.94 (C), 135.63 (C), 136.78, 137.05, 137.31, 140.64, 145.46 (C), 157.87 (C); MS (MALDI-TOF): *m*/*z*: calcd for 630.2; found: 630.5 $[M - Br]^+$, 524.7 $[M - PdBr]^+$; elemental analysis calcd (%) for $C_{36}H_{35}BrN_2PdSi$ (710.09): C 60.89, H 4.97, N 3.95, Si 3.96; found C 61.00, H 4.90, N 3.99, Si 3.87.

0947-6539/02/0801-0054 $ 17.50+.50/0 *Chem. Eur. J.* **2002**, *8*, No. 1

1-Bromo-2,6-bis(hydroxymethyl)benzene *tert*-butyldimethylsilyl ether (12): A solution of $PyH\cdot Br_3$ (3.66 g, 11.44 mmol) in MeOH (30 mL) was added dropwise at room temperature to a suspension of 3,5-bis(hydroxymethyl)benzene *tert*-butyldimethylsilyl ether (**11**) (3.07 g, 11.44 mmol) and iron powder in CH_2Cl_2 (30 mL). After 1 h, the reaction mixture was filtered, washed with water (2×15 mL) and brine (2×15 mL) and dried over $MgSO_4$. The solvent was concentrated to afford the desired dialcohol **12** as a white solid (2.88 g, 73 %). ^{1}H NMR (200 MHz, $CDCl_3$, 25 °C): $\delta=$ 0.20 (s, 6H; $SiMe_2$), 0.98 (s, 9H; Si*t*Bu), 2.19 (s, 2H; O*H*), 4.67 (s, 4H; ArCH_2), 6.92 (s, 2H; Ar*H*); ^{13}C NMR (50 MHz, $CDCl_3$, 25 °C): $\delta=4.38$ ($SiMe_2$), 18.17 [Si*C*$(CH_3)_3$], 25.64 [SiC(*C*$H_3)_3$], 64.91 (Ar*C*H_2), 119.31 (C), 141.33, 155.57 (C), 164.63 (C); elemental analysis calcd (%) for $C_{14}H_{23}BrO_3Si$ (347.34): C 48.41, H 6.67, Si 8.09; found C 48.44, H 6.59, Si 8.27.

1-Bromo-2,6-bis((methylamino)methyl)benzene *tert*-butyldimethylsilyl ether (13): Et_3N (2.80 mL, 20.15 mmol) was added to a solution of **12** (1.00 g, 2.88 mmol) in CH_2Cl_2 (20 mL) under nitrogen at −78 °C and subsequently mesyl chloride (1.65 g, 1.11 mL, 14.40 mmol). The reaction was stirred for 1.5 h at this temperature and then $MeNH_2$ was bubbled through the reaction for a period of 5 min. Formation of a white precipitate was observed. The suspension was allowed to warm up to room temperature and stirred for 1 h. After this time, water was added (10 mL) and the organic layer was separated. The obtained organic layer was washed with brine (10 mL), dried over $MgSO_4$ and concentrated to afford the desired diamine **13** as a yellow oil (0.95 g, 88 %). ^{1}H NMR (200 MHz, C_6D_6, 25 °C): $\delta=0.17$ (s, 6H; $SiMe_2$), 0.99 (s, 9H; Si*t*Bu), 2.22 (br s, 6H; NCH_3), 3.71 (br m, 4H; ArCH_2), 7.07 (s, 2H; Ar*H*); ^{13}C NMR (50 MHz, C_6D_6, 25 °C): $\delta=-4.18$ ($SiMe_2$), 18.49 [Si*C*$(CH_3)_3$], 26.10 [SiC(*C*$H_3)_3$], 35.98 (N*C*H_3), 56.13 (Ar*C*H_2), 116.78 (C), 120.24, 141.51 (C), 155.37 (C).

Synthesis of macrocycles 14 and 15: Macrocycles **14** and **15** were prepared as described for **8a**, starting from **5** and **13**. Yields: 30 % for **14** and 4 % for **15**. Macrocycle **14**: ^{1}H NMR (200 MHz, C_6D_6, 25 °C): $\delta=0.11$ (s, 6H; $SiMe_2$), 0.95 (s, 9H; Si*t*Bu), 2.18 (s, 6H; NCH_3), 2.80–3.90 (br s, 8H; ArCH_2), 6.96–7.18 (m, 12H; Ar*H*), 7.53 (d, ^3J(H,H) = 7.0 Hz, 2H; Ar*H*), 7.64–7.67 (br m, 4H; Ar*H*), 8.01 (s, 2H; Ar*H*); ^{13}C NMR (75 MHz, C_6D_6, 25 °C): $\delta=-4.25$ ($SiMe_2$), 18.43 [Si*C*$(CH_3)_3$], 25.87 [SiC(*C*$H_3)_3$], 42.66 (N*C*H_3), 58.10 (Ar*C*H_2), 61.26 (Ar*C*H_2), 119.88 (C), 122.12, 127.45, 127.74 (C), 128.38, 129.71, 130.24, 135.12, 135.23 (C), 137.21, 137.73, 138.31 (C), 141.22 (C), 154.39 (C); ^{29}Si NMR (75 MHz, C_6D_6, 25 °C): $\delta=-14.28$ (Ar_4*Si*), 21.30 (*Si*O); MS (MALDI-TOF): *m*/*z*: calcd for: 732.2; found: 730.9 $[M]^+$, 649.8 $[M-Br]^+$; elemental analysis calcd (%) for $C_{42}H_{49}BrN_2OSi_2$ (733.96): C 68.73, H 6.73, N 3.82, Si 7.65; found C 68.49, H 6.85, N 3.67, Si 7.64.

Dimer **15**: ^{1}H NMR (200 MHz, C_6D_6, 25 °C): $\delta=0.09$ (s, 12H; $SiMe_2$), 0.92 (s, 18H; Si*t*Bu), 2.01 (s, 12H; NCH_3), 3.35 (s, 8H; ArCH_2), 3.51 (s, 8H; ArCH_2), 7.11–7.24 (m, 20H; Ar*H*), 7.49 (d, ^3J(H,H) = 7.8 Hz, 4H; Ar*H*), 7.59 (d, ^3J(H,H) = 7.4 Hz, 4H; Ar*H*), 7.69–7.74 (m, 8H; Ar*H*), 7.78 (s, 4H; ArH); ^{13}C NMR (75 MHz, C_6D_6, 25 °C): $\delta=-4.20$ (Si*C*H_3), 18.51 [Si*C*$(CH_3)_3$], 25.96 [SiC(*C*$H_3)_3$], 42.26 (N*C*H_3), 61.65 (Ar*C*H_2), 62.44 (Ar*C*H_2), 118.18 (C), 121.06, 128.34, 129.90 130.58, 134.65 (C), 135.10 (C), 135.77, 136.96 (2 × ArH), 137.38, 139.19 (C), 140.55 (C), 155.28 (C); ^{29}Si NMR (75 MHz, C_6D_6, 25 °C): $\delta=-13.55$ (Ar_4*Si*), 21.61 (*Si*O); MS (MALDI-TOF): *m*/*z*: calcd for: 1467.9; found: 1468.0 $[M]^+$, 1387.7 $[M-Br]^+$.

Synthesis of ligand 16: Tetrabutylammonium fluoride (1M, 0.04 mL, 0.04 mmol) was added to a solution of **14** (0.20 g, 0.03 mmol) in THF (5 mL). The reaction was stirred at room temperature for 1 h. After this time, the solvent was removed in vacuo and the residue was dissolved in CH_2Cl_2 (10 mL), washed with a saturated aqueous solution of NH_4Cl (5 mL) and brine (5 mL), dried over $MgSO_4$ and evaporated to dryness. The phenol **16** was obtained as a white powder (160 mg, 85 %) which was crystallized by diffusion of pentane into a concentrated solution of **16** in CH_2Cl_2. ^{1}H NMR (200 MHz, C_6D_6, 25 °C): $\delta=2.21$ (s, 6H; NCH_3), 2.80–3.90 (br m, 8H; ArCH_2), 6.56 (s, 2H; Ar*H*), 7.01–7.22 (m, 10H; Ar*H*), 7.58 (d, ^3J(H,H) = 6.8 Hz, 2H; Ar*H*), 7.70 (br m, 4H; Ar*H*), 8.04 (s, 2H; Ar*H*); ^{13}C NMR (75 MHz, $CDCl_3$, 25 °C): $\delta=42.76$ (NCH_3), 57.63 (ArCH_2), 60.65 (ArCH_2), 117.02, 117.82 (C), 126.94, 127.62, 129.34, 129.98, 134.60, 136.32 (C), 136.37 (C), 136.67, 137.23, 137.46 (C), 140.39 (C), 154.13 (C); MS (MALDI-TOF): *m*/*z*: calcd for: 619.7; found: 619.3 $[M]^+$, 539.2 $[M-Br]^+$; elemental analysis calcd (%) for $C_{36}H_{35}BrN_2OSi$ (619.67): C 69.78, H 5.69, N 4.52, Si 4.53; found C 69.86, H 5.63, N 4.40, Si 4.68.

Synthesis of dendrimer 18: Et_3N (0.20 mL, 1.44 mmol) was added to a solution of **16** (67 mg, 0.11 mmol) in THF (5 mL) under nitrogen at room temperature. The reaction mixture was stirred for 15 min and then 1,3,5-benzenetricarboxylic acid chloride (91 mg, 0.03 mmol) was added. The resulting solution was allowed to stir overnight. After this time, the solvent was removed in vacuo, the residue was dissolved in CH_2Cl_2 (10 mL) and washed with water (5 mL) and brine (5 mL). The organic layer was then dried with $MgSO_4$ and evaporated to afford **18** as a white solid (61 mg, 88 %). ^{1}H NMR (200 MHz, C_6D_6, 25 °C): $\delta=2.20$ (s, 18H; NCH_3), 2.80–3.90 (br m, 24H; ArCH_2), 7.04–7.22 (m, 30H; Ar*H*), 7.28 (s, 6H, Ar*H*), 7.55 (d, ^3J(H,H) = 6.8 Hz, 6H; Ar*H*), 7.70 (br m, 12H; Ar*H*), 7.93 (s, 6H; Ar*H*), 9.50 (s, 3H, Ar*H*); ^{13}C NMR (75 MHz, C_6D_6, 25 °C): $\delta=42.87$ (NCH_3), 58.36 (ArCH_2), 60.73 (ArCH_2), 123.16, 124.82 (C), 126.67 (C), 126.98 (C), 127.22 (C), 129.77, 130.43, 131.85 (C), 135.14, 135.27, 136.12 (C), 137.19, 137.69, 137.96, 141.77, 149.46 (C), 163.09 (C=O); MS (MALDI-TOF): *m*/*z*: calcd for 2015.1; found: 2123.9 $[M+Ag]^+$, 2014.3 $[M]^+$, 1934.6 $[M-Br]^+$; elemental analysis calcd (%) for $C_{117}H_{105}Br_3N_6O_6Si_3\cdot\frac{1}{2}CH_2Cl_2$ (2142.6): C 66.43, H 5.08, N 3.92; found C 66.28, H 5.19, N 3.56.

Synthesis of dendrimer 1: $[Pd(dba)_2]$ (66 mg, 0.11 mmol) was added to a stirred solution of **18** (59 mg, 0.03 mmol) in toluene (10 mL). The resulting solution was heated under reflux overnight, during which time the color changed from deep purple to yellow. The reaction mixture was diluted with CH_2Cl_2, filtered through Celite and the solvent removed under reduced pressure. The solid residue was dissolved in CH_2Cl_2 (5 mL) and hexanes were added in order to precipitate the product. The precipitate was purified by washing first with hexane (2×20 mL) and then with Et_2O (20 mL) to afford **1** as yellow powder (40 mg; 60 %). ^{1}H NMR (300 MHz, C_6D_6, 25 °C): $\delta=2.75-2.84$ (m, 6H; ArCH_2 and 18H; NCH_3), 2.92 (d, ^3J(H,H) = 15.0 Hz, 6H; ArCH_2), 3.81 (d, ^3J(H,H) = 15.0 Hz, 6H; ArCH_2), 4.32 (d, ^3J(H,H) = 12.6 Hz, 6H; ArCH_2), 6.40 (d, ^3J(H,H) = 6.3 Hz, 6H; Ar*H*), 6.80–6.82 (m, 6H; Ar*H*), 7.03–7.16 (m, 24H; Ar*H*), 7.38 (s, 6H; Ar*H*), 7.68 (m, 12H; Ar*H*), 7.84–7.87 (m, 6H; Ar*H*), 9.44 (s, 3H; Ar*H*), 10.02 (s, 6H; Ar*H*); ^{13}C NMR (50 MHz, C_6D_6, 25 °C): $\delta=52.60$ (*C*H_3), 67.05 (Ar*C*H_2), 69.60 (Ar*C*H_2), 113.26, 123.15, 127.91, 128.59, 129.82 (C), 130.02, 131.83 (C), 132.19 (C), 133.22, 133.87 (C), 134.60, 134.85 (C), 135.72 (C), 136.76, 137.15, 137.29, 140.66, 146.13, 148.48 (C), 154.65 (C), 163.31 (C=O); MS (MALDI-TOF): *m*/*z*: calcd for 2254.5; found: 2254.9 $[M-Br]^+$, 2148.8 $[M-PdBr]^+$, 1961.6 $[M-2(PdBr)]^+$; elemental analysis calcd (%) for $C_{117}H_{105}Br_3N_6O_6Pd_3Si_3\cdot3C_6H_6$ (2568.8): C 63.12, H 4.83, N 3.27; found C 63.05, H 4.12, N 3.31.

Procedure for the Pd^{II}-catalyzed aldol reaction: The following is an example of the experimental conditions used for the Pd^{II} catalyzed aldol condensation reaction. A suspension of **10** (10 mg, 0.016 mmol) and $AgBF_4$ (4 mg, 0.020 mmol) in CH_2Cl_2 (5 mL) was stirred for ca. 30 min at room temperature. The resulting cloudy solution was filtered through Celite. Solvent was removed under reduced pressure to give the active catalyst which was dissolved in CH_2Cl_2 (5 mL). To this solution were sequentially added benzaldehyde (173 mg, 1.63 mmol), diisopropylethylamine (21 mg, 0.16 mmol) and methyl α-isocyanoacetate (161 mg, 1.62 mmol). The mixture was stirred at room temperature for 24 h. From the clear and completely homogeneous, stirred reaction mixture samples (0.1 mL) were taken after regular time intervals and analyzed by ^{1}H NMR spectroscopy in $CDCl_3$ after *careful* removal of the solvent. ^{1}H NMR (300 MHz, $CDCl_3$, 25 °C): $\delta=3.19$ (s, 3H, CO_2CH_3, *cis* isomer), 3.83 (s, 3H, CO_2CH_3, *trans* isomer), 4.62 (dd, ^3J(H,H) = 7.8, ^4J(H,H) = 2.2 Hz, 1H; -C*H*CO_2Me, *trans* isomer), 5.08 (dd, ^3J(H,H) = 11.1, ^4J(H,H) = 1.8 Hz, 1H; -C*H*CO_2Me, *cis* isomer), 5.68 (d, ^3J(H,H) = 7.8 Hz, 1H; ArC(*H*)O), 5.73 (d, ^3J(H,H) = 11.1 Hz, 1H; ArC(*H*)O), 7.11 (d, ^3J(H,H) = 2.2 Hz, 1H; *H*C=N *trans* isomer, other signal not visible due to overlap), 7.22–7.43 (m, 11H; Ar*H*).

Crystal structure determinations: X-ray intensities were measured on a Nonius KappaCCD diffractometer with rotating anode ($\lambda=0.71073$ Å) at a temperature of 150(2) K. The structures were solved with the automated Patterson program DIRDIF[32] (compound **10**) and the direct methods programs SIR97[33] (compound **16**) and SHELXS97[34] (compounds **8a**, **8b**, and **14**). The structures were refined with SHELXL97[35] against F^2 of all reflections. Non-hydrogen atoms were refined with anisotropic displacement parameters, hydrogen atoms were refined as rigid groups. Structure calculations, checking for higher symmetry and preparations of molecular plots were performed with the PLATON[36] package. Further experimental details are given in Table 4.

Table 4. Crystallographic data for the compounds **8a**, **8b**, **10**, **14**, **16**.

	8a	**8b**	**10**	**14**	**16**
formula	$C_{36}H_{35}BrN_2Si$	$C_{36}H_{36}N_2Si$	$C_{36}H_{35}BrN_2PdSi$	$C_{42}H_{49}BrN_2OSi_2$	$C_{36}H_{35}BrN_2OSi$[37]
M_W	603.66	524.76	710.06	733.92	619.66
crystal size [mm^3]	$0.50 \times 0.25 \times 0.09$	$0.45 \times 0.29 \times 0.21$	$0.38 \times 0.38 \times 0.25$	$0.35 \times 0.18 \times 0.11$	$0.30 \times 0.30 \times 0.18$
crystal colour	pale yellow	colourless	yellow	colourless	colourless
crystal system	triclinic	triclinic	monoclinic	monoclinic	monoclinic
space group	$P\bar{1}$ (No. 2)	$P\bar{1}$ (No. 2)	$P2_1/c$ (No. 14)	$P2_1/c$ (No. 14)	$C2/c$ (No. 15)
a [Å]	9.9087(4)	9.9722(1)	11.3370(4)	11.3853(1)	27.7378(3)
b [Å]	11.6169(5)	12.1487(2)	13.7887(5)	11.8896(1)	18.5891(1)
c [Å]	14.4548(5)	13.2232(1)	19.4084(7)	29.2089(2)	15.7505(1)
α [°]	67.583(2)	82.8613(7)	90	90	90
β [°]	88.335(2)	71.5698(8)	92.3084(9)	95.5501(4)	120.0925(4)
γ [°]	79.043(2)	74.0779(6)	90	90	90
V [Å^3]	1508.36(10)	1460.27(3)	3031.51(19)	3935.38(5)	7026.67(10)
Z	2	2	4	4	8
ρ [g cm^{-3}]	1.329	1.193	1.556	1.239	1.172[37]
μ [mm^{-1}]	1.430	0.108	1.998	1.139	1.232[37]
abs. correction	PLATON[36] (MULABS)	PLATON[36] (MULABS)	PLATON[36] (MULABS)	none	none
transmission	0.78 – 0.87	0.94 – 0.99	0.60 – 0.72	–	–
measured refl.	13623	30139	21404	98696	76492
unique refl.	6887	6512	6924	9028	8051
param./restraints	363/0	354/0	372/0	440/0	374/0
$R1/wR2$ (all refl.)	0.0523/0.0864	0.0427/0.0973	0.0390/0.0746	0.0437/0.0854	0.0453/0.0975
$R1/wR2$ (obs. refl.)	0.0375/0.0805	0.0367/0.0933	0.0307/0.0717	0.0332/0.0804	0.0405/0.0947
GoF	1.031	1.026	1.085	1.021	1.093
ρ (max/min) [e$^-$ Å^{-3}]	− 0.43/0.35	− 0.27/0.28	− 0.59/0.51	− 0.40/0.30	− 0.51/0.50

Crystallographic data (excluding structure factors) for the structures reported in this paper have been deposited with the Cambridge Crystallographic Data Centre as supplementary publication no. CCDC 162098 (**8a**), 162099 (**8b**), 162100 (**10**), 162101 (**14**), and 162102 (**16**). Copies of the data can be obtained free of charge on application to CCDC, 12 Union Road, Cambridge CB2 1EZ, UK (fax: (+44) 1223-336-033; e-mail: deposit@ccdc.cam.ac.uk).

Acknowledgements

We wish to thank Prof. A. Canty and Dr. S. Williams for helpful discussions during the preparation of this manuscript. G. Rodríguez thanks the Ministerio de Educación y Cultura (Spain) for a postdoctoral fellowship and the European Commission for a TMR Grant (Contract No. HPMF-CT-1999-00236). This work was supported by the Council for Chemical Sciences of the Netherlands Organization for Scientific Research (CW-NWO).

[1] G. Newkome, C. N. Moorefield, F. Vögtle, *Dendritic Molecules-Concepts, Syntheses, Perspective*, VCH, Weinheim, **1996**.

[2] For recent reviews on dendritic molecules, see: a) R. Kreiter, A. W. Kleij, R. J. M. Klein Gebbink, G. van Koten, *Top. Curr. Chem.* **2001**, *217*, 163 – 199; b) G. Newkome, E. He, C. N. Moorefield, *Chem. Rev.* **1999**, *99*, 1689 – 1746; c) A. W. Bosman, H. M. Janssen, E. W. Meijer, *Chem. Rev.* **1999**, *99*, 1665 – 1688; d) J.-P. Majoral, A.-M. Caminade, *Chem. Rev.* **1999**, *99*, 845 – 880; e) H. Frey, C. Lach, K. Lorenz, *Adv. Mater.* **1998**, *10*, 279 – 293; f) C. Gorman, *Adv. Mater.* **1998**, *10*, 295 – 309; g) A. Archut, F. Vögtle, *Chem. Soc. Rev.* **1998**, *27*, 233 – 240; h) F. Zeng, S. Zimmerman, *Chem. Rev.* **1997**, *97*, 1681 – 1712; i) D. Gudat, *Angew. Chem.* **1997**, *109*, 2039 – 2043; *Angew. Chem. Int. Ed. Engl.* **1997**, *36*, 1951 – 1955.

[3] See for example: a) M. A. Hearshaw, J. R. Moss, *Chem. Commun.* **1999**, 1 – 8; b) C. M. Cardona, A. E. Kaifer, *J. Am. Chem. Soc.* **1998**, *120*, 4023 – 4024; c) P. Ceroni, F. Paolucci, C. Parasisi, A. Juris, S. Rofia, S. Serroni, S. Campagna, A. J. Bard, *J. Am. Chem. Soc.* **1998**, *120*, 5480 – 5487; d) I. Cuadrado, C. M. Casado, B. Alonso, M. Morán, J. Losada, V. Belsky, *J. Am. Chem. Soc.* **1997**, *119*, 7613 – 7614.

[4] See for example: a) C. Köllner, B. Pugin, A. Togni, *J. Am. Chem. Soc.* **1998**, *120*, 10274 – 10275; b) M. T. Reetz, G. Lohmer, R. Schwickardi, *Angew. Chem.* **1997**, *109*, 1559 – 1562; *Angew. Chem. Int. Ed. Engl.* **1997**, *36*, 1526 – 1529; c) T. Marquardt, U. Lüning, *Chem. Commun.* **1997**, 1681 – 1682; d) J.-J. Lee, W. T. Ford, J. A. Moore, Y. Li, *Macromolecules* **1994**, *27*, 4632 – 4634.

[5] J. W. J. Knapen, A. W. van der Made, J. C. De Wilde, P. W. M. N. van Leeuwen, P. Wijkens, D. M. Grove, G. van Koten, *Nature* **1994**, *372*, 659 – 663.

[6] a) M. Albrecht, G. van Koten, *Angew. Chem.* **2001**, *113*, 3866 – 3898; *Angew. Chem. Int. Ed.* **2001**, *40*, 3750 – 3781; b) M. P. H. Rietveld, D. M. Grove, G. van Koten, *New J. Chem.* **1997**, *21*, 751 – 771, and references therein; c) G. van Koten, *Pure Appl. Chem.* **1989**, *61*, 1681 – 1694.

[7] a) A. W. Kleij, R. A. Gossage, R. J. M. Klein Gebbink, N. Brinkman, E. J. Reyerse, U. Kragl, M. Lutz, A. L. Spek, G. van Koten, *J. Am. Chem. Soc.* **2000**, *122*, 12112 – 12124; b) A. W. Kleij, R. A. Gossage, J. T. B. H. Jastrzebski, J. Boersma, G. van Koten, *Angew. Chem.* **2000**, *112*, 176 – 178; *Angew. Chem. Int. Ed.* **2000**, *39*, 176 – 178; c) R. A. Gossage, J. T. B. H. Jastrzebski, J. van Ameijde, S. J. E. Mulders, A. J. Brouwer, R. M. J. Liskamp, G. van Koten, *Tetrahedron Lett.* **1999**, *40*, 1413 – 1416; d) A. W. Kleij, H. Kleijn, J. T. B. H. Jastrzebski, W. J. J. Smeets, A. L. Spek, G. van Koten, *Organometallics* **1999**, *18*, 268 – 276; e) M. Albrecht, G. van Koten, *Adv. Mater.* **1999**, *11*, 171 – 174; f) M. Albrecht, R. A. Gossage, A. L. Spek, G. van Koten, *Chem. Commun.* **1998**, 1003 – 1004; g) P. J. Davies, D. M. Grove, G. van Koten, *Organometallics* **1997**, *16*, 800 – 802.

[8] See for example: a) R. Breinbauer, E. N. Jacobsen, *Angew. Chem.* **2000**, *112*, 3750 – 3753; *Angew. Chem. Int. Ed.* **2000**, *39*, 3604 – 3607; b) D. de Groot, E. B. Eggeling, J. C. de Wilde, H. Kooijman, R. J. van Haaren, A. W. van der Made, A. L. Spek, D. Vogt, J. N. H. Reek, P. C. J. Kamer, P. W. N. M. van Leeuwen, *Chem. Commun.* **1999**, 1623 – 1624; c) K. Vassilev, W. T. Ford, *Polym. Prepr.* **1998**, *39*, 322 – 323; d) T. Suzuki, Y. Hirokawa, K. Ohtake, T. Shibata, K. Soai, *Tetrahedron: Asymmetry* **1997**, *8*, 4033 – 4040.

[9] See for example: a) P. B. Rheiner, H. Sellner, D. Seebach, *Helv. Chim. Acta* **1997**, *80*, 2027 – 2032; b) C. C. Mak, H.-F. Chow, *Macromolecules*

1997, *30*, 1228–1230; c) D. Seebach, R. E. Marti, T. Hintermann, *Helv. Chim. Acta* **1996**, *79*, 1710–1740; d) P. Bhyrappa, J. K. Young, J. S. Moore, K. S. Suslick, *J. Am. Chem. Soc.* **1996**, *118*, 5708–5711.
[10] P. B. Rheiner, D. Seebach, *Chem. Eur. J.* **1999**, *5*, 3221–3236.
[11] H. Brunner, *J. Organomet. Chem.* **1995**, *500*, 39–46.
[12] H.-F. Chow, C. C. Mak, *J. Org. Chem.* **1997**, *62*, 5116–5127.
[13] We are also interested in the linkage between different branches of the dendrimer with the concomitant formation of cages where the reactions would take place, and therefore, the size and structure of the cavity would determine the reaction products.
[14] a) J. M. Longmire, X. Zhang, M. Shang, *Organometallics* **1998**, *17*, 4374–4379; b) M. A. Stark, C. J. Richards, *Tetrahedron Lett.* **1997**, *38*, 5881–5884; c) R. Nesper, P. Pregosin, K. Püntener, M. Wörle, A. Albinati, *J. Organomet. Chem.* **1996**, *507*, 85–101; d) F. Gorla, A. Togni, L. M. Venanzi, A. Albinati, F. Lianza, *Organometallics* **1994**, *13*, 1607–1616; e) R. Nesper, P. S. Pregosin, K. Püntener, M. Wörle, *Helv. Chim. Acta* **1993**, *76*, 2239–2249; f) T. Hayashi, M. Sawamura, Y. Ito, *Tetrahedron* **1992**, *48*, 1999–2012.
[15] See for example: a) S. Höger, A.-D. Meckenstock, S. Müller, *Chem. Eur. J.* **1998**, *4*, 2423–2434; b) V. Hensel, K. Lützow, J. Jacob, K. Gessler, W. Saenger, A.-D. Schüter, *Angew. Chem.* **1997**, *109*, 2768–2770; *Angew. Chem. Int. Ed. Engl.* **1997**, *36*, 2654–2655; c) Y. Nagasaki, E. Honzawa, M. Kato, K. Kataoka, T. Tsuruta, *Chem. Lett.* **1993**, 1825–1828; d) M. A. Pérez, J. M. Bermejo, *J. Org. Chem.* **1993**, *58*, 2628–2630; e) N. A. Porter, B. Lacher, V. H.-T. Chang, D. R. Magnin, B. T. Wright, *J. Am. Chem. Soc.* **1988**, *110*, 3554–3560; f) S. Warwel, H. Kätker, C. Rauenbusch, *Angew. Chem.* **1987**, *99*, 714–715; *Angew. Chem. Int. Ed. Engl.* **1987**, *26*, 702–703.
[16] a) B. K. Vriesema, J. Buter, R. M. Kellogg, *J. Org. Chem.* **1984**, *49*, 110–113; b) W. H. Kruizinga, R. M. Kellogg, *J. Am. Chem. Soc.* **1981**, *103*, 5183–5189.
[17] L. A. van de Kuil, H. Luitjes, D. M. Grove, J. W. Zwikker, J. G. M. van der Linden, A. M. Roelofsen, L. W. Jenneskens, W. Drenth, G. van Koten, *Organometallics* **1994**, *13*, 468–477.
[18] Prolonged addition did not afford higher yields.
[19] a) P. L. Alsters, P. J. Baesjou, M. D. Janssen, H. Kooijman, A. Sicherer-Roetman, A. L. Spek, G. van Koten, *Organometallics* **1992**, *11*, 4124–4135; b) S. Komiya, *Synthesis of Organometallic Compounds*, Wiley, Chichester, **1997**.
[20] a) H. P. Dijkstra, P. Steenwinkel, D. M. Grove, M. Lutz, A. L. Spek, G. van Koten, *Angew. Chem.* **1999**, *111*, 2322–2324; *Angew. Chem. Int. Ed.* **1999**, *38*, 2185–2288; b) P. Steenwinkel, R. A. Gossage, T. Maunula, D. M. Grove, G. van Koten, *Chem. Eur. J.* **1998**, *4*, 763–768.
[21] In the centrosymmetric unit cell, two isomers are observed. The *RS* isomer shown in Figure 2a, and its *SR* enantiomer.
[22] a) M.-C. Lagunas, R. A. Gossage, A. L. Spek, G. van Koten, *Organometallics* **1998**, *17*, 731–741; b) J. Terheijden, G. van Koten, F. Muller, D. M. Grove, K. Vrieze, *J. Organomet. Chem.* **1986**, *315*, 401–417.
[23] H. Dijkstra, M. D. Meijer, J. Patel, R. Kreiter, G. P. M. van Klink, M. Lutz, A. L. Spek, A. Canty, G. van Koten, *Organometallics* **2001**, *20*, 3159–3168.
[24] a) J. A. M. van Beek, G. van Koten, G. P. C. M. Dekker, E. Wissing, M. C. Zoutberg, C. H. Stam, *J. Organomet. Chem.* **1990**, *394*, 659–678; b) J. Terheijden, G. van Koten, J. A. M. van Beek, B. K. Vriesema, R. M. Kellogg, M. C. Zoutberg, C. H. Stam, *Organometallics* **1987**, *6*, 89–93.
[25] A. M. Clark, C. E. F. Richard, W. R. Roper, L. J. Wright, *Organometallics* **1998**, *17*, 4535–4537.
[26] Molecular modelling was performed using MMFF94, Spartan 5.1, SGI.
[27] U. Kragl, C. Dreisbach, *Angew. Chem.* **1996**, *108*, 684–685; *Angew. Chem. Int. Ed. Engl.* **1996**, *35*, 642–664.
[28] D. M. Grove, G. van Koten, J. N. Louwen, J. G. Noltes, A. L. Spek, H. J. C. Ubbels, *J. Am. Chem. Soc.* **1982**, *104*, 6609–6616.
[29] This is important to note as the precipitated silver salt can also act as a Lewis acid catalyst.
[30] J. Brunner, F. M. Richards, *J. Biol. Chem.* **1980**, *255*, 3319–3329.
[31] Amination of **12** with Me_2NH gave the dimethylamino analogues of **13**. Further deprotection, acylation with AcCl and oxidative addition of $[Pd(dba)_2]$ afforded compound **20** in 44% overall yield.
[32] P. T. Beurskens, G. Admiraal, G. Beurskens, W. P. Bosman, S. Garcia-Granda, R. O. Gould, J. M. M. Smits, C. Smykalla, *The DIRDIF97 program system*, Technical Report of the Crystallography Laboratory, University of Nijmegen (The Netherlands), **1997**.
[33] A. Altomare, M. C. Burla, M. Camalli, G. L. Cascarano, C. Giacovazzo, A. Guagliardi, A. G. G. Moliterni, G. Polidori, R. Spagna *J. Appl. Crystallogr.* **1999**, *32*, 115–119.
[34] G. M. Sheldrick, *SHELXS97*, *Program for crystal structure solution*, University of Göttingen (Germany), **1997**.
[35] G. M. Sheldrick, *SHELXL97*, *Program for crystal structure refinement*, University of Göttingen (Germany), **1997**.
[36] A. L. Spek, *PLATON*, *A multipurpose crystallographic tool.* Utrecht University (The Netherlands), **2001**.
[37] The crystal structure of compound **16** contains large voids (1325.9 $Å^3$ per unit cell) filled with disordered solvent molecules. Their contribution to the structure factors was secured by back-Fourier transformation using the routine CALC SQUEEZE of the program PLATON[35] (144 electrons/unit cell). Derived values (formula weight, density, absorption coefficient) do not contain the contribution of the disordered solvent.

Received: May 21, 2001 [F3272]